Geologic Map 79

Geologic map of the Valles caldera, Jemez Mountains, New Mexico

Fraser Goff
Jamie N. Gardner
Steven L. Reneau
Shari A. Kelley
Kirt A. Kempter
John R. Lawrence

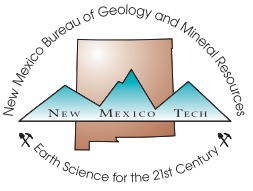

New Mexico Bureau of Geology and Mineral Resources
A division of New Mexico Institute of Mining and Technology

Socorro 2011

Geologic map of the Valles caldera, Jemez Mountains, New Mexico

by

Fraser Goff, Jamie N. Gardner, Steven L. Reneau, Shari A. Kelley,
Kirt A. Kempter, and John R. Lawrence

PROJECT MANAGEMENT & EDITING
Jane C. Love
L. Greer Price

GRAPHICS
Leo Gabaldon
Phil Miller

CARTOGRAPHY
Rebecca Titus Taylor

LAYOUT & DESIGN
Julie Hicks

A division of New Mexico Institute of Mining and Technology

Daniel H. López, *President*
801 Leroy Place
Socorro, NM 87801
(575) 835-5145
www.geoinfo.nmt.edu

ISBN 978-1-883905-29-3

This volume is dedicated to U.S. Senator Jeff Bingaman and former U.S. Senator Pete Domenici, who worked together to ensure the preservation of these geologically significant lands for posterity.

Printed in the United States of America

First Printing July 2011

Geologic map of the Valles caldera, Jemez Mountains, New Mexico

Fraser Goff

Department of Earth and Planetary Sciences, University of New Mexico, Albuquerque, New Mexico 87131

Jamie N. Gardner

14170 NM–4, Jemez Springs, New Mexico 87025

Steven L. Reneau

Earth and Environmental Sciences Division, Los Alamos National Laboratory, Los Alamos, New Mexico 87545

Shari A. Kelley

New Mexico Bureau of Geology and Mineral Resources, New Mexico Institute of Mining and Technology, 801 Leroy Place, Socorro, New Mexico 87801

Kirt A. Kempter

2623 Via Caballero del Norte, Santa Fe, New Mexico 87505

John R. Lawrence

Lawrence GeoServices Ltd. Co., 2321 Elizabeth St. NE, Albuquerque, New Mexico 87112

Introduction

Smith et al. (1970) published the first color geologic map of the entire Jemez Mountains at 1:125,000 scale. At the center of this map is their geologic depiction of the Valles caldera based on many decades of field work. The map immediately became a popular resource for researchers and students of geology and related sciences because of Valles caldera's fame as a model for large resurgent calderas. This small-scale map still remains an excellent visual tool for field trips and regional geologic uses. However, the celebrity of Valles caldera and the Jemez Mountains attracted many more researchers after 1970. Refinements to the geology were published on unit names, unit ages, unit subdivisions, interpretations of processes, etc. Additionally, geothermal drilling and geophysical investigations from roughly 1970 to 1983 revealed that the cross sections of Smith et al. needed thorough revisions (Goff 1983; Goff et al. 1989). Soon after the Valles Caldera National Preserve (VCNP) was created in 2000, the preserve trustees realized that a detailed geologic map and up-to-date cross sections of the caldera were required for future land use planning, resource management, and evaluation of geothermal resources. Volcanologists have needed an updated map that uses modern geochronologic and geochemical techniques to provide structural and temporal frameworks for assessing caldera models and volcanic hazards. Seismologists need a more detailed geologic map and sections to evaluate hazards and to more accurately locate earthquakes and interpret subsurface data. Hydrologists need an up-to-date map to identify and manage water resources. Climate modelers want a map that details the age and duration of intracaldera lakes. And the population of northern New Mexico has grown substantially in the last 50 years, making the resources and potential hazards of the Valles caldera regionally significant. Thus, at the invitation of VCNP and with part-time funding from Los Alamos National Laboratory, the first three authors began to remap the geology of the Valles caldera at 1:24,000 scale in spring 2002. By 2004 funding sources expanded to several state and federal agencies, and many additional field geologists joined the effort.

Our present 1:50,000-scale color geologic map of Valles caldera is printed on a shaded relief base. Researchers and students can download the same 1:50,000-scale map on a standard topographic base from the New Mexico Bureau of Geology and Mineral Resources Web site, http://geoinfo.nmt.edu/publications/maps/geologic/gm/79. The map includes all or parts of nine U.S. Geological Survey topographic quadrangles covering approximately 306 mi^2 (804 km^2) (Fig. 1). The nine larger-scale maps (1:24,000) that were the source for this compilation were produced as open-filed geologic maps with the bureau's STATEMAP Program and are available for download from the bureau's Web site using the links provided in the reference list. These larger-scale digital maps do not reflect all of the updates apparent on this printed compilation. This multi-purpose map is intended to be a fundamental tool for professional research as well as a source of information for the non-professional visitor. As such, the first sections of this report are aimed at the interested visitor, whereas the remainder of the discussions and map unit descriptions are intended for the professional.

Physical Setting

The Valles caldera lies in the center of the Jemez Mountains, a large volcanic field that has been built over the last 14 million years in north-central New Mexico. Valles caldera gets its name from Spanish for the many spectacular valleys within it, the largest of which are Valle Grande, Valle San Antonio, Valle Toledo, and Valle de los Posos (Fig. 2). Topographically, Valles caldera is bounded by the La Grulla Plateau to the northwest, Tschicoma Peak to the northeast, the Sierra de los Valles to the east, Frijoles and Medio Dia Canyons to the southeast, Aspen Ridge, Paliza Canyon, and Los Griegos to the south, Cañon de San Diego to the southwest, and the Jemez Plateau to the west. Three important perennial streams have

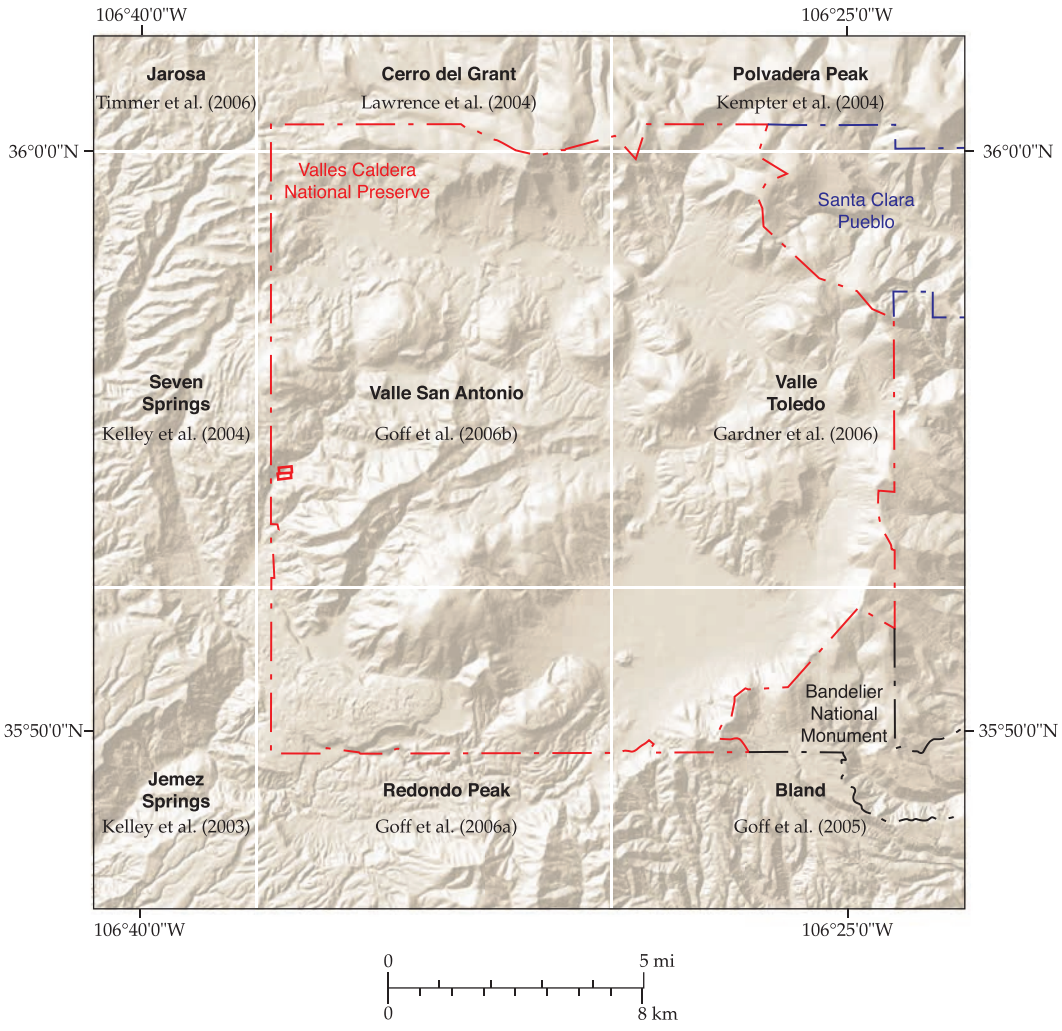

FIGURE 1—Key to the new geologic quadrangle maps used to construct this map.

their headwaters in the Valles caldera. The East Fork Jemez River drains the eastern and southern caldera, whereas San Antonio Creek drains the northern and western portions of the caldera. These streams join at Battleship Rock to form the Jemez River, which flows southwest down Cañon de San Diego toward the village of Jemez Springs. Santa Clara Creek heads near Cerro Toledo and drains the northern part of the Toledo embayment in the northeast caldera region, flowing east through Santa Clara Pueblo. Highest elevations in the Valles region are at Redondo Peak (11,254 ft), in the approximate center of the caldera, and at Tschicoma Peak (11,561 ft) just northeast of the caldera. Lowest elevations in the map area are in the Rito de los Frijoles (approximately 7,200 ft) southeast of the caldera and the Jemez River (approximately 6,800 ft) southwest of the caldera. Visitors should be aware, however, that NM–4 traverses the southern part of the caldera at altitudes mostly over 8,000 ft, and in places over 9,000 ft, above sea level.

Valles Caldera in Society and Science

The Valles caldera is more than a spectacularly beautiful place. The geology and resources of the Valles caldera have had significant impacts on society and science for a long time, and likely will continue to do so for years to come.

History

Valles caldera was inhabited originally by pre-Columbian Indian cultures (Paleo-Indian, Archaic, and ancestral Puebloan), whose members hunted and fished the valleys and surrounding slopes and mined obsidian from Cerro del Medio, mostly during spring, summer, and fall, since about 10,000 years ago. Archaeological analyses have established broad regional use of Valles caldera obsidians through geochemical characterization of glasses at Cerro del Medio, Rabbit Mountain, and other nearby sources (Baugh and Nelson 1987; Glascock et al. 1999; Shackley 2005; Steffen 2005). Surrounding modern pueblos have very strong cultural bonds to the caldera and especially to Redondo Peak and Cerro Toledo. In 1876, 28 years after the conclusion of war between the United States and Mexico, the United States delivered title of the Baca Location No. 1 land grant, which includes most

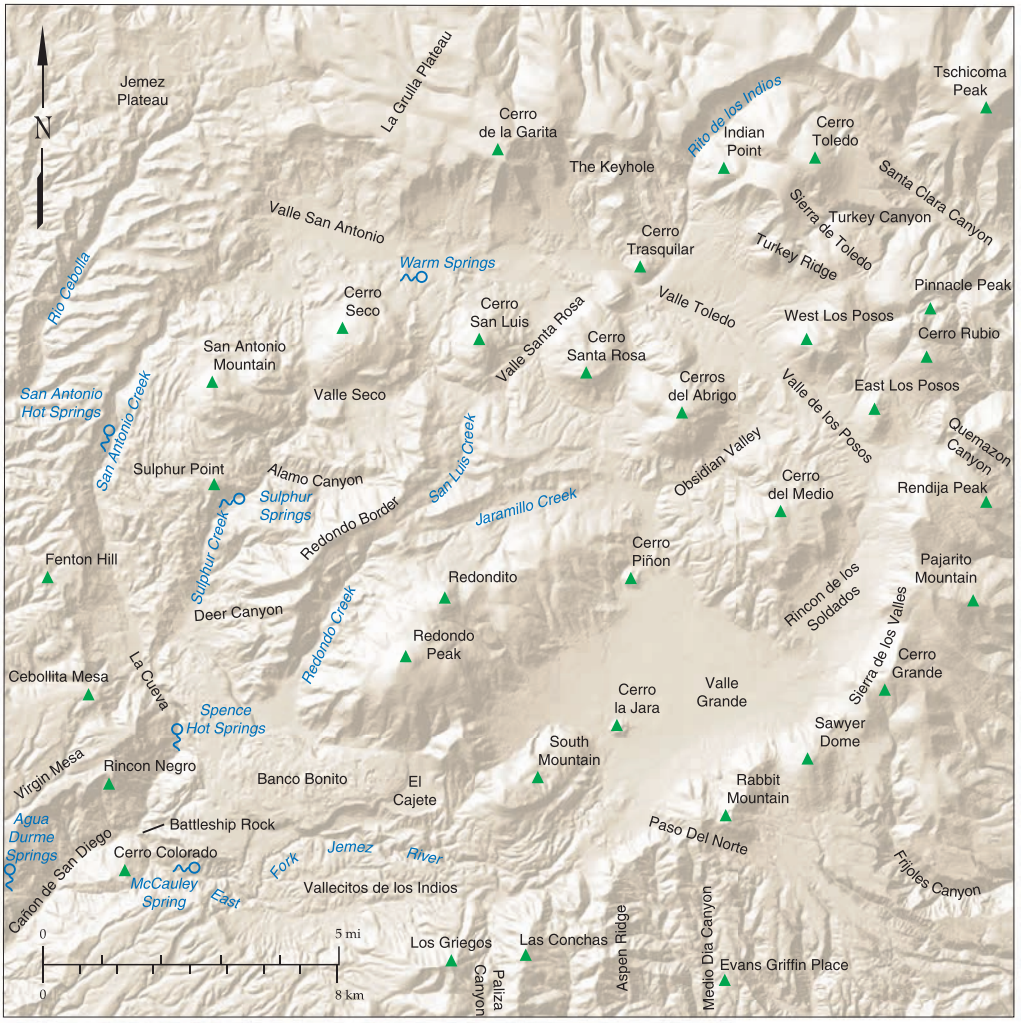

FIGURE 2—Place names and physiographic features used on this map.

of Valles caldera, to the heirs of Luis Maria Cabeza de Baca who had ranched in northern New Mexico since at least 1821 (Martin 2003; Anschuetz and Merlan 2007). At that time, the Baca No. 1 consisted of nearly 99,300 acres. Private ownership of "the Baca" changed hands several times until it was sold in 1963 to J. P. "Pat" Dunigan (Abilene, Texas) for $2.5 million. By that time, the Baca was essentially surrounded by Santa Fe National Forest. Elk from Wyoming were successfully introduced to the Baca in 1947 and 1964. In the summer of 2000, the federal government bought the Baca ranch property from the Dunigan heirs for $106 million and created the Valles Caldera National Preserve (VCNP) by act of Congress. Occupying most of the Valles caldera, VCNP is a special land unit of more than 88,000 acres administered by a presidentially appointed board of trustees. Bandelier National Monument abuts the southeast boundary of VCNP, and a few small private in holdings (for example, Sulphur Springs and Vallecitos de los Indios) are to the west, south, and southeast of the preserve.

Volcanology

Valles caldera is the world's premier example of a resurgent caldera, a giant circular volcano with an uplifted central floor. Smith and Bailey (1968) published a generalized model of caldera formation that is based on their work on "the Valles," and it is reverently taught in most volcanology classes to this day. The Valles caldera consists of a 13.6-mi- (22-km-) diameter collapse depression containing a central elliptical dome (Redondo Peak) and a near-perfect ring of roughly 15 postcaldera lava dome and flow eruptions (Figs. 2 and 3). Valles and the earlier, nearly coincident Toledo caldera formed at 1.25 and 1.64 Ma[1], respectively, during two explosive events that erupted huge pyroclastic flows whose deposits are collectively named the Bandelier Tuff. So much material was erupted so rapidly that, in each case, a large void at the top of the emptied magma chamber developed. The crust overlying the emptied magma chamber caved in, leaving the bowl-shaped crater of the caldera as the surface expression of the plan view of the magma chamber. Renewed magma pressure from below uplifted the floor of the caldera to form the resurgent dome (Redondo Peak) within a few tens of thousands of years of

[1]ka, Ma—Throughout this text numerical ages of geologic units, whether determined by radioactive-decay rates or other processes, are expressed using the abbreviations ka and Ma for kilo-annum, 10^3 years, and mega-annum, 10^6 years, (recommended International System of Units convention). For example, the very young Banco Bonito Flow may have erupted as recently as 34,000 years ago, and its age is commonly written as 34 ka. The age of the 1,250,000-year-old Tshirege Member of the Bandelier Tuff is shown as 1.25 Ma.

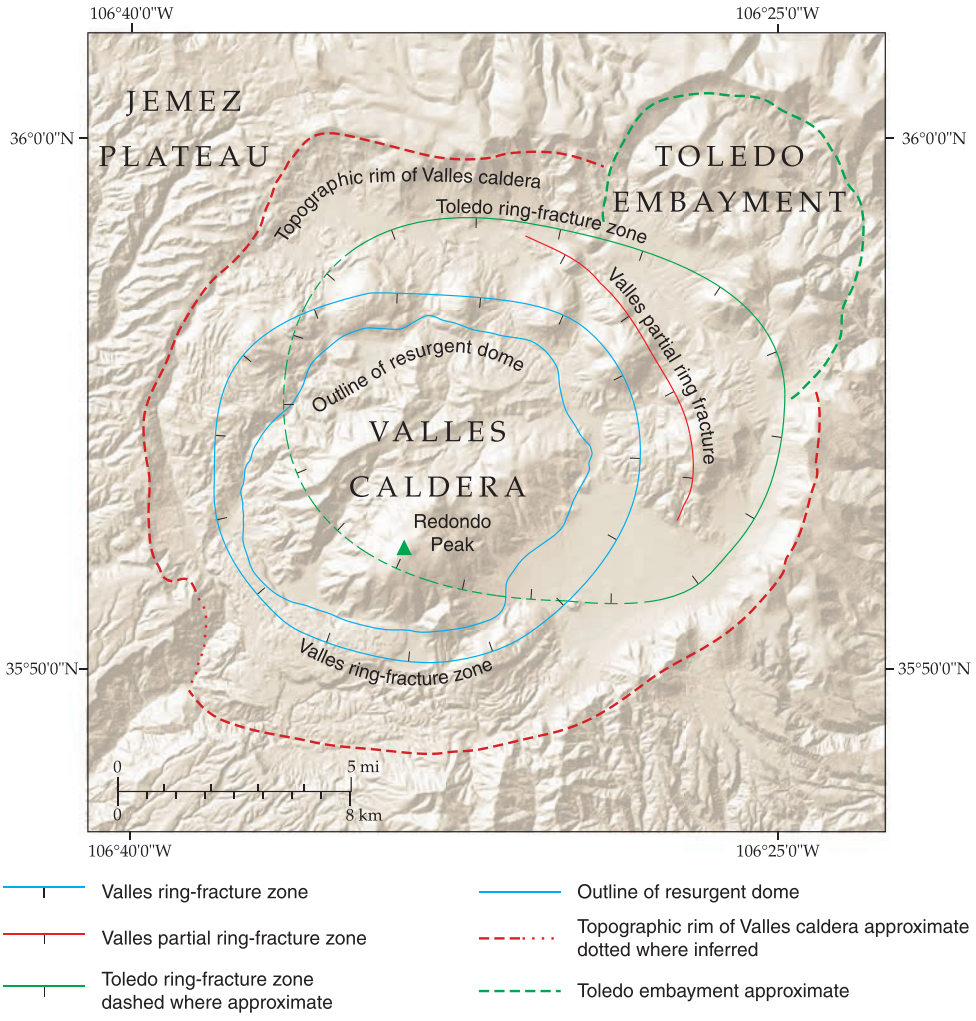

FIGURE 3—Map showing the locations of the Toledo and Valles ring-fracture zones.

caldera formation. Relatively smaller, episodic eruptions continued within the caldera, forming the ring of postcaldera lava domes and flows (map). This model for the development of a resurgent caldera has served as the global standard for other calderas, and has facilitated recognition and understanding of calderas around the world. Smith and Bailey (1966) also determined that the composition of the Bandelier Tuff varies systematically from top to bottom, being more enriched in silica, quartz, and other constituents at the bottom than at the top. From this work they determined that the Bandelier magma chamber was compositionally zoned. Zoned magma chambers have now been documented at many other caldera sites worldwide.

The oldest ring-fracture eruption since formation of Valles caldera is the dome complex of Cerro del Medio (about 1.2 million years ago), and the youngest eruption is the Banco Bonito lava flow erupted about 40,000 years ago (Gardner et al. 2010). Many volcanoes developed within the Valles between these two eruptions. The Valles caldera cycle is merely the latest volcanic episode of the Jemez Mountains volcanic field, which has erupted to form lava flows, lava domes, and pyroclastic deposits for the last 14 million years (Gardner et al. 1986; Self et al. 1986; Goff and Gardner 2004; Kelley et al. in prep.).

Volcanic hazards

The model of caldera formation and evolution, developed by Smith and Bailey (1968) based on their work on the Valles caldera, is of far greater than simply academic importance. Armed with this model, volcanologists gained many insights on the stages of development of other calderas. No two volcanoes are exactly alike, but the Valles model gave researchers working on other calderas an idealized plan of what to look for and expect. In particular, this led to recognition and vastly improved understanding of two other young caldera systems in the western United States: Long Valley caldera in eastern California, and Yellowstone in Wyoming. Both of these caldera systems exhibit remarkable similarities to the Valles caldera and are presently monitored for impending eruptions.

And how about the Valles itself? Will it erupt again? The answer is an emphatic "yes," with the main uncertainty not *if* but *when* it will erupt. It has been recognized for some time that magma exists beneath the Valles at depths as shallow as 3 mi (5 km) (Steck et al. 1998). Additionally, some researchers have made the case that the youngest eruptions from the caldera (from 60,000 to 40,000 years ago) represent a fresh magma batch, unrelated to any earlier magmas, and that some possible precursors to volcanic activity may be indicating

impending eruptions (Wolff and Gardner 1995; Reneau et al. 1996). Based on available evidence, another huge caldera-forming eruption is unlikely. Far more probable are smaller, but still potentially explosive, eruptions similar to those that happened at Valles 60,000–40,000 years ago. For an idea of scale, these smaller eruptions were quite similar to the famous eruptions of Vesuvius (Italy) in 79 A.D. that buried the towns of Pompeii and Herculenium. Consequences of such an event in the Valles caldera would likely be localized, small-volume pyroclastic flows within the caldera and its stream drainages, volcanic dome building, localized flooding, and widespread ash fall outside of the caldera.

Geothermal resources

Valles caldera contains a classic, liquid-dominated hydrothermal system (575°F) that was heavily explored and drilled for geothermal energy production from the mid-1960s to 1983 (Dondanville 1978; Grant et al. 1984; Truesdell and Janik 1986). Many hot springs and fumaroles within the caldera (≤195°F) are manifestations of the underlying geothermal resource, notably the acid solfatara at Sulphur Springs and the popular bathing sites at Spence, McCauley, and San Antonio Springs (Goff and Grigsby 1982; Goff et al. 1985). The deepest well in the caldera, Baca-12, is about 10,500 ft (3,200 m) deep, bottoming in relatively impermeable Precambrian quartz monzonite (650°F) beneath Redondo Creek (Nielson and Hulen 1984). The Baca geothermal project never successfully produced electricity, to the dismay of the U.S. geothermal industry (Kerr 1982; Goldstein and Tsang 1984). In contrast, three scientific holes drilled into the caldera from 1984 to 1988 produced a wealth of information on intracaldera stratigraphy, configuration of the hydrothermal system, and high-temperature slim hole coring and logging techniques (Goff et al. 1988; Gardner et al. 1989; Lysne and Jacobson 1990; Goff and Gardner 1994).

The world's first hot dry rock (HDR) geothermal system, a series of experiments to mine heat from hot, impermeable rock, was engineered beneath Fenton Hill on the southwest margin of Valles caldera (Heiken et al. 1981; Murphy et al. 1981). Four holes as deep as 2.8 mi (4.5 km) were drilled in hot (615°F) Precambrian crystalline rocks to determine how to extract heat (e.g., well EE-2, map; Laughlin et al. 1983). Although these experiments proved the technical feasibility of HDR, a commercial system was never successfully developed at Fenton Hill for a number of reasons (Kerr 1987; Brown and Duchane 1999). However, the concepts and technology from Fenton Hill have been exported to several other countries, and the first commercial HDR system (now called EGS, enhanced geothermal systems) will probably succeed at the Soultz site in France (Gérard et al. 2006).

Ore deposit analogs

The close association of many ore deposits with volcanoes and their hydrothermal fluids has been commented upon for years, perhaps centuries (e.g., White 1955; Sillitoe and Bonham 1984; Elston 1994). Small quantities of sulfur were mined from the altered volcanic rocks at Sulphur Springs on the western resurgent dome in the early 1900s (Summers 1976). Cores and cuttings from holes drilled in the Valles geothermal system have revealed deposition of sub-ore grade molybdenum (as MoS_2) and additional ore minerals containing silver, lead, zinc, copper, manganese, arsenic, and antimony that post-date emplacement of the Tshirege Member of the Bandelier Tuff (Hulen and Nielson 1986, 1988; Hulen et al. 1987; WoldeGabriel and Goff 1989; 1992; Goff and Gardner 1994). These minerals are associated with gangue constituents (quartz, calcite, pyrite, etc.) common in volcano-hosted ore deposits. Fluids trapped in vein quartz during crystallization ("fluid inclusions") have salinities and entrapment temperatures resembling salinities and reservoir temperatures in the present geothermal system (Hulen et al. 1987; Sasada and Goff 1995). Thus, the Valles ore minerals were precipitated from fluids similar to those presently circulating in the caldera, and the Valles caldera is a modern analog of ore processes encountered at many eroded calderas (Bethke and Rye 1979).

Plate tectonics

Valles caldera played a significant role in the plate tectonic revolution of the 1960s (Glen 1982) by having some volcanic rocks of perfect ages to provide crucial tests of some key plate tectonic concepts. In the 1960s symmetrical stripes of alternating normal and reversed magnetic polarity were discovered on ocean floors adjacent to spreading centers like the mid-Atlantic ridge. These stripes were thought to result from flipping of the earth's magnetic field as submarine lavas were erupted and the sea floor continued to spread. Early opponents to plate tectonics argued that the magnetic anomaly patterns around mid-ocean ridges had formed by other processes, such as hydrothermal alteration. If this process is recorded in lavas on ocean floors, places must exist on the continents where magnetic reversals can be found and dated in subaerial lavas. Some of the young reversals of the earth's magnetic field found on the sea floor were discovered at three domes in the northern Valles caldera: Cerro Abrigo (normal polarity), Santa Rosa I (transitional polarity), and San Luis (reverse polarity; Doell et al. 1968). The Santa Rosa I dome erupted as the earth's magnetic field was flipping from normal to reverse polarity. This work ultimately resulted in the naming of the Jaramillo normal event at around 1 Ma (after Jaramillo Creek) and the Santa Rosa transitional event at about 0.94 Ma (Glen 1982; Singer and Brown 2002). Thus, the Valles caldera provided confirmation of some fundamental plate tectonic concepts, especially sea-floor spreading, leading to widespread acceptance of the theory that has unified previously disparate aspects of geosciences, affording, among other things, powerful predictive capabilities regarding regions prone to earthquakes and volcanoes.

Climate cycles

Lake basins and their deposits record variable climate conditions for periods that may exceed a million years. Sediments, pollen, and paleomagnetic signals are indicators of conditions that prevail in the area surrounding the lake (e.g., Davis 1998). In the late 1940s a number of wells were drilled into Valle Grande to assess possible water resources for (at that time) the "new" city of Los Alamos, and the wells penetrated as much as 295 ft (90 m) of lacustrine beds (Conover et al. 1963). Pollen samples taken from sediments in one well formed the partial basis for an early study on climate cycles (Sears and Clisby 1952), but the work was done when carbon-14 dating was only in its infancy and, in the absence of age constraints for the pollen, was nearly forgotten. With renewed interest in climate change and climate models, the lacustrine beds beneath Valle Grande were cored in May 2004 to determine their cause, duration, and climate variability (Fawcett et al. 2007, 2011; Donohoo-Hurley et al. 2007). Approximately 260 ft (80 m) of mostly lacustrine silty mud was recovered. An ash bed at the bottom of the lacustrine sequence was dated at 0.55 ka, similar to the age of South Mountain lava dome indicating the lake

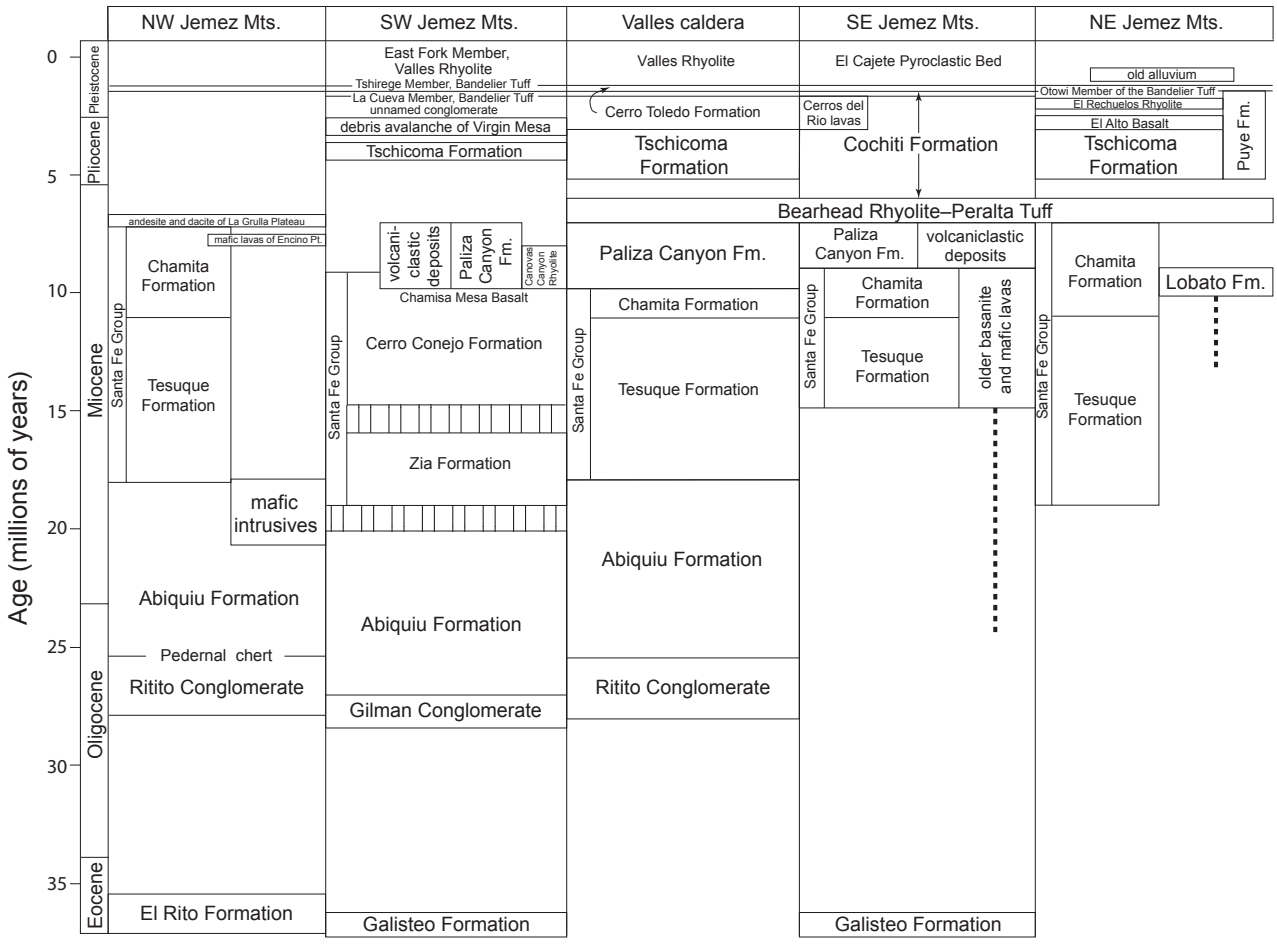

FIGURE 4—Chart showing regional and older stratigraphic units of the Jemez Mountains (from Gardner et al. 2010, fig. 3).

formed when the lava dammed the East Fork Jemez River. Correlation of climate changes in the core with other long climate records and identification of geomagnetic polarity events that appear to be dated global events show that the core spans two glacial-interglacial cycles in the mid-Pleistocene lasting about 200,000 years. Thus, Valle Grande contains the longest known Pleistocene lake record in the southwestern USA (Fawcett et al. 2007, 2011).

Stratigraphy

Our map contains revisions to stratigraphy based on 40 years of recent study (Gardner et al. 2010; Kelley et al. in prep.). Fundamentally, the volcanic rocks of the Jemez Mountains are now part of two stratigraphic groups, Keres and Tewa (Fig. 5). The Keres Group comprises nearly all precaldera volcanic units in the Jemez Mountains (Fig. 5). The Tewa Group includes volcanic rocks and deposits related to the evolution of the Valles and Toledo caldera complex, and includes the three formations Bandelier Tuff, Cerro Toledo Formation, and Valles Rhyolite.

Those who conduct research in the Jemez Mountains and Valles caldera may find the following list of changes useful when comparing our map with the previous maps and studies of the Jemez Mountains volcanic field (for example, Smith et al. 1970 and Bailey et al. 1969).

Bland intrusive rocks: The Bland intrusive (unit *Tm*) and volcanic rocks surrounding the Cochiti mining district southeast of the caldera are included within the Paliza Canyon Formation as first recognized by Stein (1983). Our mapping shows that the Bland volcanics are altered Paliza Canyon volcanics (Goff et al. 2005, 2006a) intruded by monzonite and quartz monzonite stocks, dikes, sills, and plugs.

La Grulla Formation: A new unit has been created, the La Grulla Formation, which lies on the northwest flank and wall of the caldera (Kelley et al. 2007a; Rowe et al. 2007). The La Grulla Formation (roughly 8–7 Ma) consists of basalt, andesite, and dacite that have transitional chemistry between slightly alkalic compositions in the Paliza Canyon Formation (mostly >7 Ma) and calc-alkaline rocks in the Tschicoma Formation (mostly <6 Ma).

Bearhead Rhyolite: The Bearhead Rhyolite extends from the southeastern to the northeastern Jemez Mountains, a much greater aerial distribution than previously recognized. Although this extended distribution was recognized by both

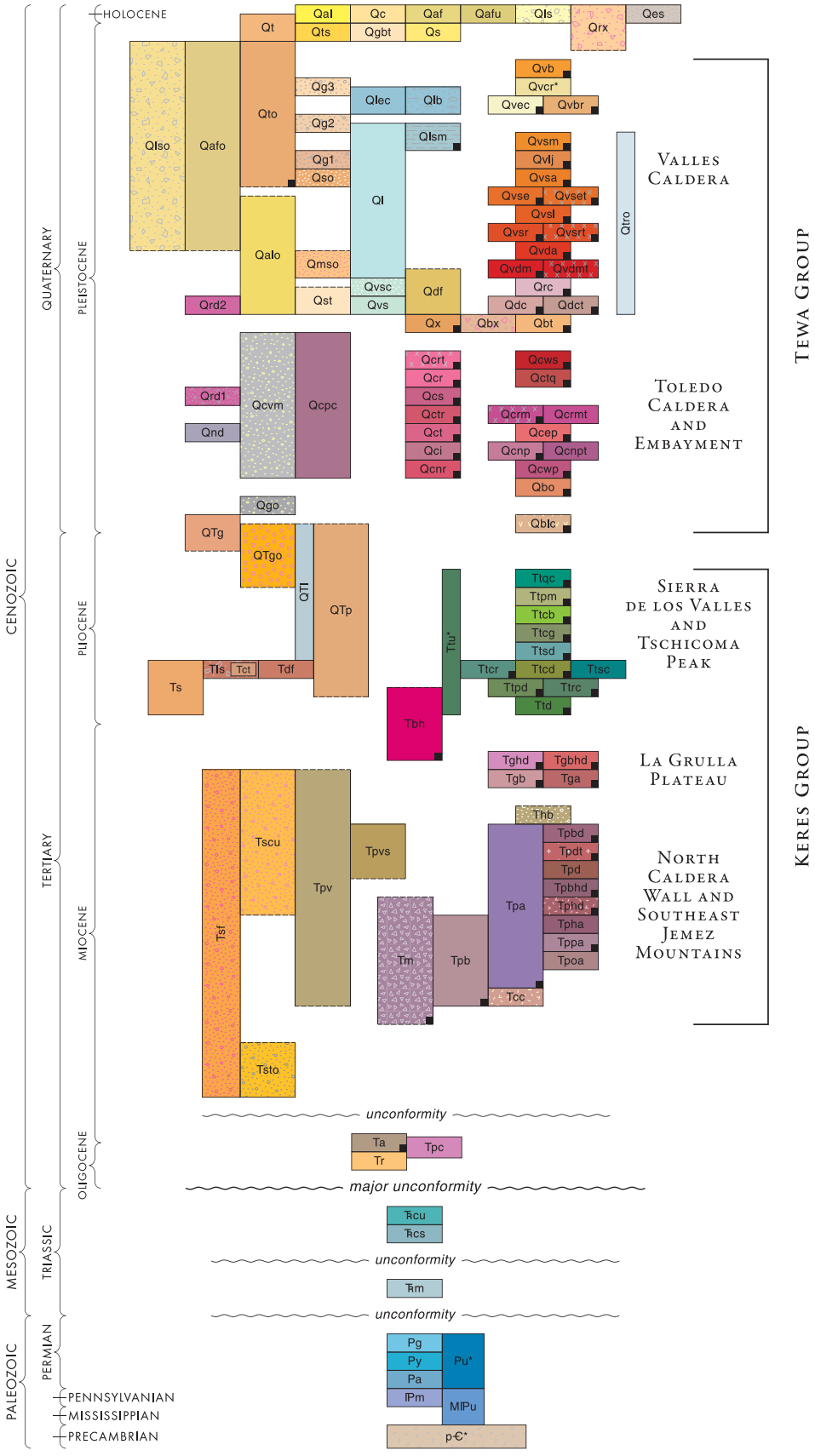

FIGURE 5—Correlation chart of map and cross section units in the Valles caldera region, New Mexico. Asterisk (*) denotes units shown on cross sections only. Black square denotes dated unit.

Gardner et al. (1986) and Loeffler et al. (1988), recent mapping shows that Bearhead rocks crop out as flows, domes, dikes, sills, and pods on the north flank of the caldera and in the north caldera wall, west of the Toledo embayment (Kempter et al. 2004; Gardner et al. 2006; Goff et al. 2006b).

Cerro Rubio Quartz Latite: The Cerro Rubio Quartz Latite, originally mapped as a plug and dome in the Toledo embayment (Griggs 1964; Bailey et al. 1969; Smith et al. 1970) is no longer afforded formation status. The rocks that constitute the former formation are now considered part of the precaldera Tschicoma Formation because they are temporally and chemically similar to those rocks (Gardner et al. 1986; Stix et al. 1988; Gardner and Goff 1996; Gardner et al. 2010).

La Cueva Member, Bandelier Tuff: The La Cueva Member of the Bandelier Tuff is now formalized to distinguish the relatively small volume, high-silica rhyolite ignimbrites that pre-date the Otowi Member (Self et al. 1986; Kelley et al. 2007b; Gardner et al. 2010). The new member eliminates terms such as pre-Bandelier tuffs, San Diego Canyon ignimbrites, lower tuffs, and "swept-under-the-carpet tuffs" used by a variety of researchers since the early 1980s.

Cerro Toledo Formation: The rhyolite domes, flows, and tephras composing the Cerro Toledo Rhyolite are now part of the Valle Toledo Member of the Cerro Toledo Formation (Gardner et al. 2010). Most of the domes are now uniquely named due to petrographic and age differences (Stix et al. 1988). Warm Springs, Cerro Trasquilar, West and East Los Posos, and Paso del Norte rhyolites are now included within the Valle Toledo Member because their eruption ages are between those of the Otowi and Tshirege Members of the Bandelier Tuff (between 1.64 and 1.25 Ma).

Valles Rhyolite: The Valle Grande Member of the Valles Rhyolite has been abandoned because of widespread disuse and lack of utility (Gardner et al. 2010). However, the Valles Rhyolite now includes several new members reflecting individual eruptive complexes along the Valles ring-fracture zone. Each dome complex is subdivided into eruptive units or pulses where possible. The former members Banco Bonito, El Cajete, and Battleship Rock have been reduced in stratigraphic stature to become part of the new East Fork Member of the Valles Rhyolite. They are now formally called the Banco Bonito Flow, the El Cajete Pyroclastic Beds, and the Battleship Rock Ignimbrite (Gardner et al. 2010; Wolff et al. 2011).

Toledo Caldera and Embayment

Mapping, other surface studies, geophysics, dating, and drilling have been combined to show the approximate position of the Toledo caldera and ring-fracture zone (Fig. 3; Goff et al. 1984; Heiken et al. 1986; Self et al. 1986; Stix et al. 1988; Spell et al. 1996; Gardner et al. 2010). Most of Toledo caldera has been obliterated by the younger Valles caldera. Four domes, (west to east) Warm Springs, Cerro Trasquilar, and two Los Posos domes (1.5–1.25 Ma; map) define a remnant arc of the Toledo ring-fracture zone in northern Valles caldera. These domes were formerly depicted as post-Valles in age (Smith et al. 1970). More recent mapping strongly suggests that other ring-fracture rhyolite vents of the Toledo caldera are obscured and/or obliterated by the younger Valles caldera. Rabbit Mountain (1.43 Ma), a Toledo ring-fracture rhyolite on the east flank of Valles caldera, is merely a preserved fragment of what was a much larger dome and flow complex. Paso del Norte dome (1.47 Ma) is also a partial remnant of what was probably a much larger dome and flow complex. The position of the southwestern Toledo ring-fracture zone shown in Figure 3 is slightly speculative but incorporates recent interpretations of Bandelier Tuff stratigraphy presented by Warren et al. (2007).

The new geologic map has not unambiguously resolved the age and origin of the semicircular feature northeast of Valles caldera, now called the Toledo embayment (Goff et al. 1984; the former Toledo caldera identified by Smith et al. 1970). Various age constraints limit formation of the Toledo embayment between 2.3 and 1.5 Ma (Gardner and Goff 1996). The cross sections presented on the map imply that the Toledo embayment is a feature that formed slightly later than the Toledo caldera during eruption of a cluster of Valle Toledo Member domes, but other interpretations are possible. For example, Gardner and Goff (1996) argue that the embayment formed during the collapse of the Toledo caldera along a structurally controlled zone that hosted a northeasterly elongated offshoot from the main Toledo caldera magma body. At odds with other researchers (e.g., Self et al. 1986; Hulen et al. 1991), Nowell (1996) interprets the gravity low beneath the Toledo embayment as a shallow residual magma body of Tschicoma Formation age and suggests that the embayment is a buried vent for La Cueva Member ignimbrites.

Valles Resurgent Dome

Geothermal and scientific drilling from 1960 to 1988 and gravity data obtained in the early 1970s show that intracaldera Bandelier Tuff is thicker in the central and eastern caldera than was previously thought by Smith et al. (1970). This is reflected in their cross sections, which show only 1,000–2,000 ft (300–600 m) of collapse. The near perfect symmetry of Valles caldera masks the very strong northeast trends of major faults, gravity gradients and other structural elements of the caldera, and progressive piecemeal collapse of the caldera floor to the southeast. The new information shows that there is anywhere from 2,000 to 8,200 ft (600 to 2,500 m) of collapse going from west to east, a reflection of preexisting Rio Grande rift structure. This revelation has many consequences for how the resurgent dome rocks are interpreted and mapped.

Caldera collapse breccias (megabreccias)

In their landmark paper on resurgent calderas, Smith and Bailey (1968) did not appreciate the amount of collapse that can take place during caldera formation. As a result, large fragments of precaldera rocks shown as faulted blocks within the resurgent dome portion of their map (Smith et al. 1970) are actually caldera-collapse breccia (megabreccia) blocks (*Qx*). These are a combination of caldera-wall collapse breccias as

traditionally defined by Lipman (1976), breccias from piecemeal foundering of the Valles caldera floor, and breccia blocks recycled from the previous Toledo caldera. The collapse-breccia concept explains how Bandelier Tuff encapsulates blocks of various older rock types. By and large, megabreccia blocks of Pennsylvanian to Permian age are concentrated in the north and west sectors of the resurgent dome. Younger megabreccia blocks (Tertiary to Quaternary) are found in the east and south. This distribution of ages probably reflects rock depths and thicknesses in precaldera units filling and straddling an early Rio Grande rift.

Deer Canyon Member

The new map breaks out lava units of the Deer Canyon Member (*Qdc*) from tuffaceous units (*Qdct*) and identifies several locations of Deer Canyon rocks not previously shown. This member consists of the first rhyolitic products erupted after formation of Valles caldera (Bailey et al. 1969; Smith et al. 1970). High-precision $^{40}Ar/^{39}Ar$ dating shows that Deer Canyon rocks are indistinguishable in age from the youngest member of the Bandelier Tuff (both about 1.25 Ma; Phillips et al. 2007). Generally speaking Deer Canyon lavas are porphyritic and crystal rich in the southwestern resurgent dome and are aphyric to crystal poor in the central to northeastern resurgent dome (Goff and Gardner 2004; Goff et al. 2006b; 2007). The aphyric lavas commonly display thin, tightly folded flow bands. Deer Canyon tephras mimic the lavas in mineralogy within any given area and are commonly very lithic rich.

Redondo Creek Member

We are now calling Redondo Creek Member lavas "rhyodacite" due to their transitional chemistry and mineralogy (Goff et al. 2007). Specifically, Redondo Creek lavas contain no quartz and minor sanidine. The principal phenocrysts are plagioclase, clinopyroxene, and biotite. Silica contents generally fall between 69 and 72 wt.% SiO_2. The name change highlights the significant field and geochemical differences between Redondo Creek lavas and other postcaldera lavas.

Caldera-fill sedimentary units

Valles caldera contains a diverse assemblage of sedimentary rocks deposited early in the caldera history (Smith and Bailey 1968; Goff et al. 2007). Previously depicted as one unit (Smith et al. 1970), we have now broken the caldera fill into three units, two predominately lacustrine and fluvial units (*Qvs* and *Qvsc*) and a predominately debris-flow, talus breccia, and landslide breccia unit (*Qdf*). There are many locations on the resurgent dome where the three types interfinger, and the boundary between them becomes somewhat arbitrary. *Qvsc* is distinguished from *Qvs* by the presence of abundant detrital biotite in the former, indicating that these sediments formed during and after eruption of Redondo Creek Member lavas.

Resurgent dome faults

The Valles resurgent dome was lifted more than 3,280 ft (1,000 m) above the existing caldera floor within 27,000 ± 27,000 years of caldera formation (Phillips et al. 2007). Although the caldera floor was already broken from earlier events, such rapid uplift stretched and broke the resurgent dome into yet more large and small fault blocks. Our new mapping does not substantially change the primary fault patterns shown previously (Smith and Bailey 1968; Smith et al. 1970). However, we consider that there are three primary fault block domains (Redondo Peak block, Redondo Border block, and San Luis block) separated by three major grabens (Redondo Creek, Jaramillo Creek, and San Luis Creek) (Fig. 6; Goff et al. 2003). The Valles resurgent dome is elliptical, oriented northeast, and the major graben-bounding faults trend north to northeast following the previous structural grain of the Rio Grande rift (Goff et al. 1989).

Lake History

Intracaldera lakes are a component of the caldera model formulated by Smith and Bailey (1968). These authors describe early lake deposits accumulating immediately after caldera formation, and these deposits are now contained with units *Qvs* and *Qvsc* of the new map. Smith et al. (1970) show younger lake deposits in the caldera ring-fracture zone, particularly in Valle San Antonio and Valle Toledo. Because of recent research on Valle Grande lake deposits as proxies for climate models (Fawcett et al. 2007, 2011), various lake deposits have been broken out in the ring-fracture zone on our map (see also, Gardner et al. 2007; Reneau et al. 2007). Considerably more research should be conducted on this topic. At least five time-constrained periods of lake deposition are recognized in Valles caldera:

1. Pre- and co-resurgence lake deposits 1.25 to roughly 1.20 (?) Ma are interbedded in Deer Canyon and Redondo Creek Member lavas and tuffs on and around the flanks of the resurgent dome. These deposits commonly show zeolitic alteration, as described below.
2. 800 ka lake deposits can be found in the northern ring-fracture zone. These deposits underlie and are interbedded with the hydromagmatic tuffs of Cerro Seco (0.8 Ma). A possible beach sand deposit (unit *Qso*) overlies the northeast flank of Cerro Seco at 9,000 ft (2,750 m).
3. A long lake occupied Valle San Antonio and Valle Toledo after eruption of San Antonio Mountain rhyolite dammed San Antonio Creek at 0.56 Ma (Gardner and Goff 1996; Rogers et al. 1996; Reneau et al. 2007). This deposit locally overlies Cerro San Luis Member rhyolite (0.8 Ma; magnetically reversed). Four samples of the lacustrine deposit exposed in a landslide scar on the west side of lower Valle Santa Rosa (fig. 9 of Reneau et al. 2007) have normal magnetic polarity (F. Goff, C. J. Goff, and J. W. Geissman, unpubl. data) verifying that the lacustrine beds in this location were deposited after 760 ka. The duration of the San Antonio Lake is not known.
4. A broad lake formed in Valle Grande when South Mountain rhyolite was erupted at 0.52 Ma (Fawcett et al. 2007, 2011; Reneau et al. 2007). As mentioned above, (Climate cycles, page 5) these deposits were penetrated by several wells and have a maximum known thickness of approximately 300 ft (90 m) beneath the axis of the East Fork Jemez River (Conover et al. 1963). Research on cores obtained from the lacustrine beds in 2004 reveals the South Mountain Lake

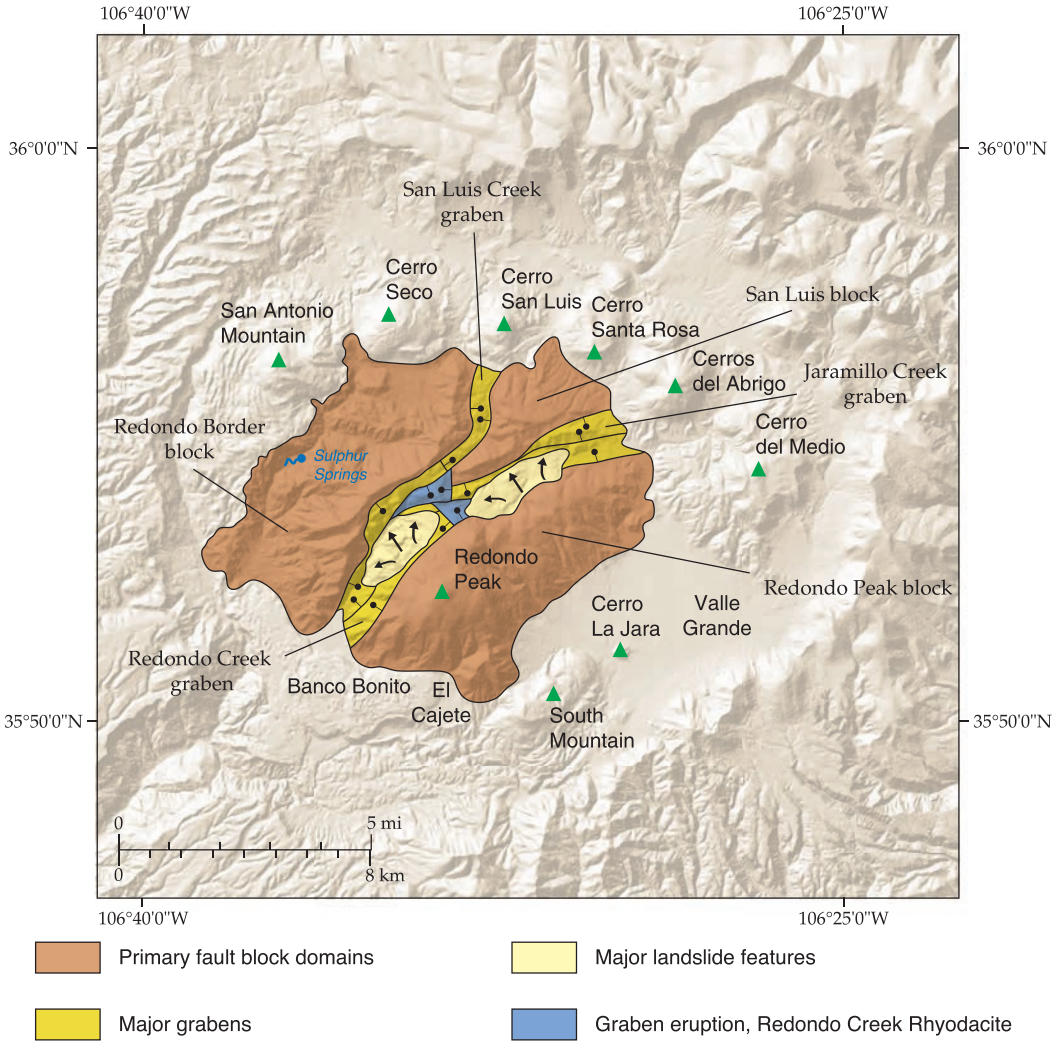

FIGURE 6—Map of resurgent dome segments and major grabens, Valles caldera.

existed over two glacial-interglacial intervals ending at about 368 ka (Fawcett et al. 2007, 2011). A section of (young?) South Mountain lake deposits is exposed in Rincon de los Soldados (unit *Qlsm*), just northeast of Valle Grande (Reneau et al. 2007, fig. 3). Paleomagnetic work on several samples from this section yields normal magnetic polarities indicating that the Rincon sediments were deposited after 760 ka (L. Donohoo-Hurley, P. Fawcett, and F. Goff, unpubl. data).

5. The last known lake in Valle Grande formed when the El Cajete vent erupted at 50–60 ka depositing a thick pumice blanket on the south side of South Mountain and damming the East Fork Jemez River (Reneau et al. 2007). Because pumice is so easily eroded, the El Cajete Lake was presumably short lived. Nonetheless, pumice-rich shoreline and bar deposits (unit *Qlec*) and small quantities of El Cajete lake deposits (unit *Qlb*) still remain around the margins of Valle Grande and Cerro La Jara.

Geomorphic Evolution of the Southern Caldera Moat

Our new mapping plus drilling of the VC-1 core hole (Gardner et al. 1987; Goff et al. 2006a) shows that several cycles of incision and backfill occurred in the southern moat of the caldera as the East Fork Jemez River cut through the southwest caldera wall and the youngest moat volcanics were periodically erupted (Fig. 7 and map). A sedimentary deposit (*Qg1*) underlies South Mountain lava in several locations along lower East Fork canyon where it overlies Tertiary andesite and Permian red beds. Most of the deposit consists of gravels, but it includes a small exposure of lacustrine beds just downstream (west) of Jemez Falls. The lava flow (*Qvsm2*) is several kilometers long and more than 100 ft (30 m) thick, and its linear shape suggests that it filled a paleocanyon existing 520 ka.

In the same general area, a second sedimentary package (*Qg2*) forms an irregular sandwich between South Mountain lava and overlying pyroclastic rocks of El Cajete pumice and Battleship Rock tuff. *Qg2* is best exposed on either side of the East Fork upstream of Jemez Falls, but roughly 85 ft (26 m) of *Qg2* is found in hole VC-1 between decomposed South Mountain flow breccia and East Fork Member tuff (map and cross section B–B´). *Qg2* is in part time equivalent to the

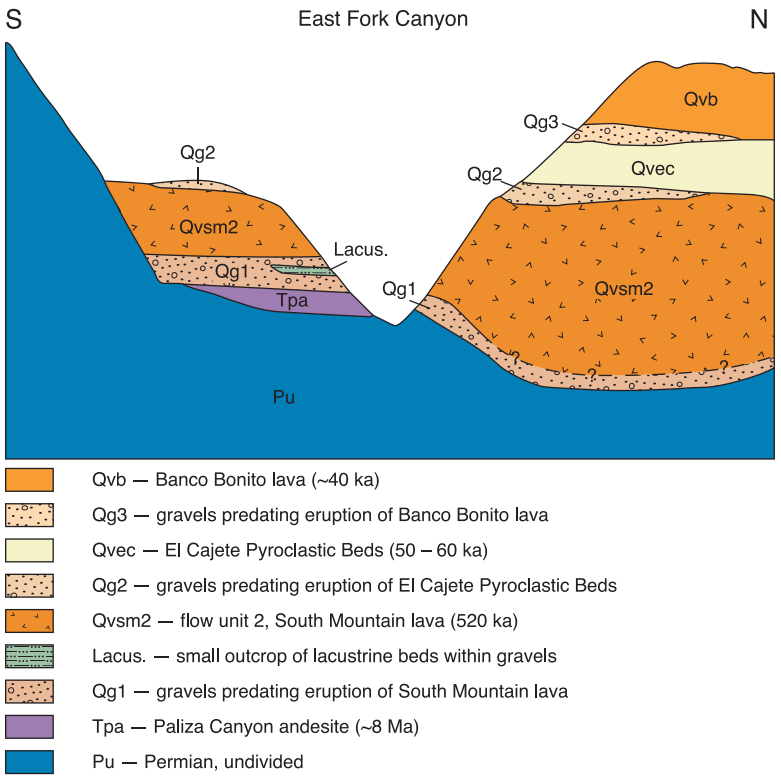

FIGURE 7—East Fork Jemez River cut through the southwest caldera wall and the youngest moat volcanics.

lacustrine rocks of the South Mountain Lake (*Qlsm*) exposed in the Valle Grande area. Stratigraphic constraints bracket the age of *Qg2* between 520 and roughly 55 ka.

A third package of gravels and sands (*Qg3*) overlies El Cajete and Battleship Rock pyroclastic beds and underlies the Banco Bonito rhyolite. This package also is exposed on either side of the East Fork upstream of Jemez Falls but south of NM–4 (map). An irregular layer of *Qg3* gravels that underlies the Banco Bonito lava is exposed west of VC-1. In these slopes, *Qg3* appears to partially fill two deep ravines cut into the underlying Battleship Rock Ignimbrite. *Qg3* is time equivalent to the El Cajete lacustrine deposits (*Qlec*) found around Valle Grande (between roughly 55 and 40 ka).

Hydrothermal Alteration

The previous map of Smith et al. (1970) made no mention of hydrothermal alteration in the Jemez Mountains other than to state that rocks in the Bland area (southeast of this map) are "chloritized" and "mineralized." Previous to 1979, alteration studies and maps showing Valles caldera were simplistic providing little information on mineral assemblages, formation temperatures, and alternation ages. Because hydrothermal alteration indicates physical and chemical conditions regarding active and past geothermal systems and ore deposits, we have constructed an alteration map of the Valles region (Fig. 8) to show specific locations and ages of alteration types.

Precaldera

Three zones along the Valles caldera walls display argillic to propylitic alteration that occurred in early to mid-Keres Group time (Fig. 8). Paliza Canyon Formation basalt and andesite in the southeast caldera wall near Las Conchas Peak are characterized by propylitic alteration (≥430°F or 220°C; quartz, calcite, chlorite, illite, epidote, pyrite) dated at 8 Ma (WoldeGabriel and Goff 1989). This grades with increasing elevation into argillic alteration (≤300°F or 150°C; epidote absent, smectite present). Hematite is found in both alteration types. This alteration style extends southeast into the Cochiti mining district where it is associated with the Bland intrusive rocks (Bundy 1958). Additional alteration as young as 5.7 Ma is focused along faults that contain quartz veins related to intrusions of Bearhead Rhyolite (WoldeGabriel and Goff 1989; Goff et al. 2005, 2006a). Similar but weaker propylitic alteration (≤430°F or 220°C; epidote generally absent) is dated between about 8 and 7 Ma in Paliza Canyon rocks exposed in the west and north caldera walls (WoldeGabriel 1990).

The rhyolite bodies in the north caldera wall intrude Keres flows and interbedded sediments tentatively correlated with the Chamita Formation (Santa Fe Group). Some of the sediments are thoroughly cemented with hematite and silica. Where this alteration is pervasive, rhyolite bodies are so silicified that the original texture and mineralogy of the

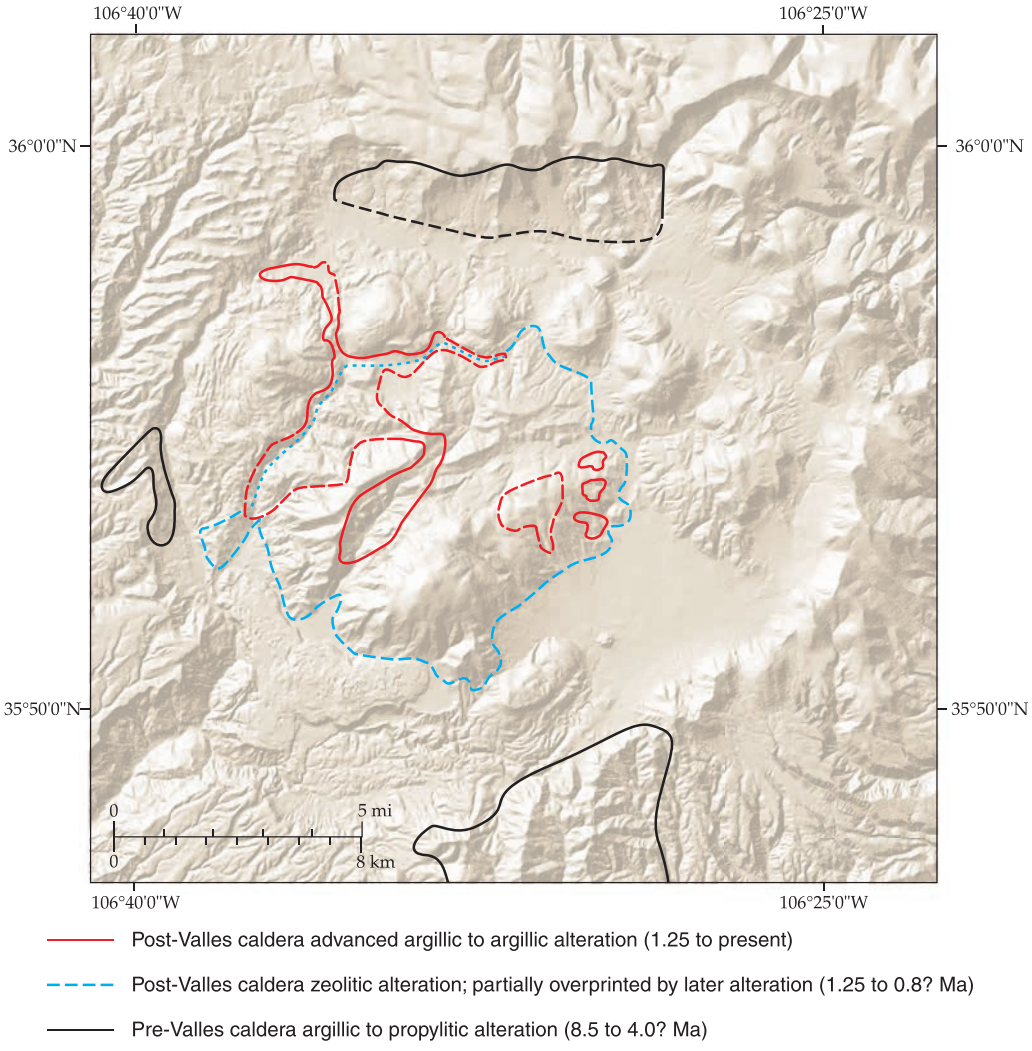

FIGURE 8—Hydrothermal alteration map of Valles caldera region.

rock is virtually destroyed. However, a fresh rhyolite dike in this zone has an age of 4.81 Ma (Kelley et al. in prep).

We have found essentially no evidence for hydrothermal activity associated with the large dome and dome complexes of Tschicoma Formation preserved east and northeast of the caldera. Possibly, Tschicoma-age alteration (5–2 Ma) would be observed if the domes were more deeply eroded. Commonly, large dacite and rhyodacite dome fields host vigorous geothermal systems that form ore deposits (Sillitoe and Bonham 1984; Elston 1994).

Postcaldera

Many of the postcaldera sediments and volcanic rocks on the resurgent dome are pervasively altered from very pale green to pale pink colors. XRD analyses show that the glass shards in the tuffs and the tuffaceous matrix of the sediments have been converted to a mixture of clinoptilolite, mordenite (both zeolites), smectite, and a silica phase, usually opal or opal CT (Chipera et al. 2007; Goff et al. 2007). The zeolite alteration, mostly ≤210°F or 100°C, is not uniform. It is most common in rocks flanking the resurgent dome, and it extends for several feet into the top of the Bandelier Tuff. Where early postcaldera sediments and volcanics have been stripped away near the crown of the resurgent dome, zeolite alteration is generally missing. Zeolite alteration is not pervasive in rocks younger than 800 ka, such as the younger lacustrine and volcanic units filling the ring-fracture zone. Thus, zeolite alteration is apparently associated with the first Valles lake(s). This lake was probably warm to hot in some locations, and slightly saline from input of hydrothermal fluids. Argillic alteration associated with soft-sediment deformation of lacustrine beds, such as observed in VC-2B (Gardner et al. 1989) is correlative with the zeolite alteration.

Silicic alteration (probably ≤300°F or 150°C) is present as veins and silicified breccias along many of the graben faults and nearby crosscutting faults in the central resurgent dome. This assemblage consists of quartz/chalcedony, pyrite, clays, and Fe-oxides, and the altered rocks represent previous conduits for deeply circulating hydrothermal fluids. The most common rock type hosting this alteration is the youngest member of the Bandelier Tuff. We have also found four small areas of eroded sinter ("geyserite," a hot spring deposit) deposits adjacent to faults. Because it is restricted to resurgent dome faults this (high-temperature?) silicic alteration apparently occurred early in the caldera history.

A zone of low-temperature silicic alteration is present in early postcaldera sediments on the northwest flank of the

resurgent dome. The alteration in this area has been barely studied and may be a residue of acid-sulfate alteration (≤210°F or 100°C). The main alteration phases are quartz and/or chalcedony, opal, sparse kaolinite, and smectite. Patches of Fe-oxides and veinlets of potassium-rich psilomelane also have been identified in this area.

Acid-sulfate alteration is widespread in the west and northwest resurgent dome and in localized parts of the northern ring-fracture zone and the Redondo Creek fault zone. This alteration is characterized by various silica phases, kaolinite, alunite, and Fe-oxides. It is widespread in the Redondo Creek lavas and associated rocks along the Sulphur Creek fault zone, but it is also in lacustrine rocks beneath Cerro Seco tuff near San Antonio Creek and in Deer Canyon ignimbrite upstream of Santa Rosa Bog (map). Thus, this alteration type has formed intermittently for possibly 1 million years or more. Present fumaroles and acid springs at Sulphur Springs, Alamo Canyon, and Redondo Creek graben are characterized by acid-sulfate alteration, but, in addition, sulfur, pyrite, jarosite, gypsum, and a host of soluble sulfates are also present (Charles et al. 1986).

Noticeably absent in all near-surface alteration assemblages are calcite and other carbonates, although they are common in the deeper parts of the hydrothermal system (Hulen and Nielson 1986; Goff and Gardner 1994). Very rarely secondary carbonate is found as cement in some near-surface, intracaldera sedimentary rocks.

As a result of these observations, our updated surface alteration map of the caldera region (Fig. 8) replaces the highly generalized maps of Doell et al. (1968) and Dondanville (1978). These authors presented all-inclusive alteration maps and did not recognize the widespread zeolite alteration (described above) or changes in alteration style that occurred with time. As one would expect, some alteration types overprint others.

Geophysical Structure

Gravity

The detailed Valles caldera gravity structure was published by Segar (1974), and reproduced and reinterpreted in some form by Nielson and Hulen (1984), Goff et al. (1989), and Nowell (1996). The basic features of these studies show: (1) a broad, circular gravity low of more than 20 mGal, more or less mimicking the topographic outline of the caldera and the Toledo embayment, (2) a large, southeast-trending increase of the gravity anomaly with the maximum low centered beneath Valle Grande, (3) abrupt gravity gradients along the margins of the caldera, and (4) a pronounced northeast trend to the subsurface gravity structure. The major conclusion from this work is that the subsurface of Valles caldera is very asymmetric, displaying relatively shallow collapse on the northwest and very deep collapse on the southeast. Because the gravity structure trends northeast, the fault pattern in the resurgent dome and the northeast position of the Toledo embayment with respect to the caldera is probably inherited from the preexisting, northeast-trending Rio Grande rift. The gravity work and drilling results formed the basis for construction of a generic northwest-southeast cross section across the caldera (Goff 1983), which was later republished by many authors.

The gravity interpretations are partially dependent on thicknesses and densities assigned to the various units (Nowell 1996). Drilling provides good controls on these variables for the southwest sector of the caldera (Nielson and Hulen 1984; Goff et al. 1989; Goff and Gardner 1994). The gravity data have never provided a satisfactory interpretation for the origin of the Toledo embayment (see Nowell 1996, p. 126). Since these studies, our recent mapping of the caldera shows that the thickness of Miocene sedimentary rocks is much greater in the northeast part of the caldera than previously thought (unit *Tscu*), and this insight is reflected in our cross sections (Cross Sections, point 2, page 14).

Seismic reflection/refraction

Seismic investigations conducted around Valles caldera have focused on finding the locations and depth to magma bodies and not resolving the upper (2 mi) 3 km of structure. The most recent seismic investigations (Steck et al. 1998; Aprea et al. 2002) conclude that an anomalously hot, more or less cylindrical mass of rock extends from roughly 3 to 4.4 mi (5 to 7 km) depth all the way to the mantle (28 mi, 45 km). This hot cylinder contains pockets and layers interpreted to be partially crystallized but still molten dikes, sills, and other intrusive bodies, and is generally centered beneath the southwestern caldera where the youngest eruptive units (East Fork Member) and geothermal system exist. The base of low-density rocks representing "caldera fill" is poorly imaged at depths of 1 to 1.5 mi (1.5 to 2.5 km), but the error on this estimate is large and no fine structure can be resolved. Thus, to date, seismic investigations reveal nothing about caldera subsidence and resurgence structure.

Drilling Constraints

Deep drilling

Drill logs with subsurface stratigraphic assignments are available for all but one of the 40+ deep geothermal wells drilled inside and around the southwest margin of the caldera (see Nielson and Hulen 1984; Goff et al. 1985; Goff et al. 1989; Goff and Gardner 1994 for logs or references to specific wells). The exception is AC-1 drilled in the central part of Alamo Canyon. The deepest well inside the caldera is Baca-12 in the southern Redondo Creek graben (approximately 2 mi, 3.2 km), whereas the deepest well outside the caldera is EE-2 drilled at Fenton Hill (approximately 2.7 mi, 4.4 km). The published stratigraphy from these wells is incorporated into the cross sections where possible and provides excellent control on thickness of the Bandelier tuffs and underlying units.

Temperature measurements

The various drill holes also provide temperature measurements as functions of depth for the central and southwestern caldera areas. Temperature measurements and gradients from shallow wells in the northeastern caldera region are summarized in Sass and Morgan (1988). Deep temperatures are

perfectly constrained to depths of 10,500 to 14,436 ft (3,200 to 4,400 m) beneath the central to southwestern margin of the caldera but are extrapolated below depths of approximately 984 ft (300 m) beneath the northeastern caldera. Because of continuing interest in geothermal energy development in the Jemez Mountains region, the temperature measurements are used to construct temperature isotherms, shown on the cross sections, from which one can infer temperatures at depth for all areas around the caldera. The isotherms shown along the west and southwest parts of the cross sections are highly accurate. The extrapolated isotherms along the northeast and east sectors of the cross sections are probably generous, slightly higher for a given depth than they really are. These data show that the temperature anomaly within Valles is highest around the Redondo Creek graben and Sulphur Springs areas and that the anomaly decreases significantly in all directions outside of the caldera.

Caldera Structure and Resurgence

Subsidence structure

Cole et al. (2005) evaluate caldera structures and models (including the Valles cross section first presented in 1983) and discuss major types of calderas. Keep in mind that Valles caldera is developed on the west margin of the preexisting Rio Grande rift with major down-to-the-east and southeast faults (Gardner et al. 1986; Goff and Gardner 2004) and that it is preceded by the comparably sized but not exactly coincident Toledo caldera (Fig. 3). Both of these earlier features provided a highly faulted and fractured terrain in which Valles caldera formed (Goff 1983; Self et al. 1986). Thus, Valles did not collapse as a simple, subsiding plate as often mistakenly portrayed (e.g., Lipman 2000, table 1). Rather, Valles collapsed as an intricate maze of already broken blocks. With our new knowledge of surrounding Tertiary sediments, many of the eastern blocks contain substantial amounts of mid-Tertiary basin fill beneath intracaldera tuffs. Thus, the large gravity anomaly beneath the southeast sector of Valles indicates the effects of previous rifting and caldera development; it does not indicate that Valles is a "trap door" caldera (Heiken et al. 1986). On this basis, Valles is best visualized as a "chaotic" piecemeal collapse caldera (Cole et al. 2005, fig. 9).

Analog models

A number of recent analog (sandbox) models (e.g., Kennedy et al. 2004; Acocella 2007) demonstrate that caldera collapse begins with development of circular, high-angle reverse faults (inner ring faults) as the caldera floor initially founders and subsides. For calderas with large eruption volumes (35 mi^3 or 150 km^3 or greater), continued subsidence forms circular, high-angle normal faults (outer ring faults) outboard of the initial reverse faults. The models show that the outer ring faults connect with the inner ring faults at depth (Acocella 2007, fig. 21). For calderas of the Valles size, the connection depth of the two types of ring faults is probably 0.6–1.2 mi (1–2 km) below surface. Furthermore, it is more than likely that the inner collapse fault (a reverse fault) becomes reactivated as a high-angle normal fault during resurgence.

Just as large-scale collapse is complex, uplift of the Valles resurgent dome should not be viewed as simple, symmetrical uplift of a broad domal plate or as a flat, rising "piston" (Nielson and Hulen 1984, fig. 17; Lipman 2000). Geologic mapping, drilling results, and gravity data show that Valles resurgence is differential and segmented. Graben orientations are strongly controlled by previous Rio Grande rift structure. In addition, the structural pattern of Valles resurgence is not caused by injection of a single immense dike or a single subjacent intrusive body (Rubin 1992; Marti et al. 1994). Instead, resurgence at Valles is caused by rise and injection of many Deer Canyon and Redondo Creek magmas into an already fragmented caldera floor (Smith and Bailey 1968). Lavas, tuffs, and vents from these eruptions are scattered all over the resurgent dome, yet none of the deep wells penetrate any intrusive bodies to depths of 10,500 ft (3,200 m) (Nielson and Hulen 1984). Thus, the depth to the tops of the crystallized stock or coalesced intrusions that cause resurgence is somewhere between 2 and 3 mi (3.2 and 5 km), the lower depth provided by seismic data mentioned above.

Resurgence timescale

From the work of Phillips et al. (2007), we now know that the Valles resurgent dome rose quickly, within 27,000 ± 27,000 years of caldera formation, confirming the early geologic reasoning of Smith and Bailey (1968). The minimum uplift of the Redondo Peak block above the caldera floor is 3,300 ft (1,000 m); thus, resurgence occurred within 54,000 years yielding a minimum uplift rate of roughly 1.9 cm/year. A faster rate is conceivable, and resurgence was no doubt episodic. For comparison, the Valles resurgence rate is similar to the resurgence rate of the presently active Ischia (Italy) caldera (3.3 cm/year) and most other dated or active resurgent domes (Phillips et al. 2007; Vezzoli et al. 2009).

Cross Sections

Our three cross sections incorporate surface observations, drilling data, and geophysical results from the past with concepts from recent analog models and our new mapping and dating. Fundamental elements of the Valles cross sections are:

1. Down-to-the east structural fabric controlled by the preexisting Rio Grande rift and the position of the previous, overlapping Toledo caldera. Tuffs of the La Cueva Member are lumped with the Otowi Member on the cross sections.
2. Chaotic, piecemeal collapse of a highly faulted basement. Precaldera, eastward thickening of the Santa Fe Group and Keres Group volcanic rocks, plus formation of earlier Toledo caldera, explains much of the observed gravity anomaly beneath Valle Grande and the Toledo embayment.
3. Paired ring faults as indicated by analog models. The inner ring faults are reverse faults during collapse, but many become reactivated as normal faults during resurgence. These reactivated normal faults bounding the margin of the resurgent dome are recognizable in the field.
4. Caldera-collapse breccias of several origins.

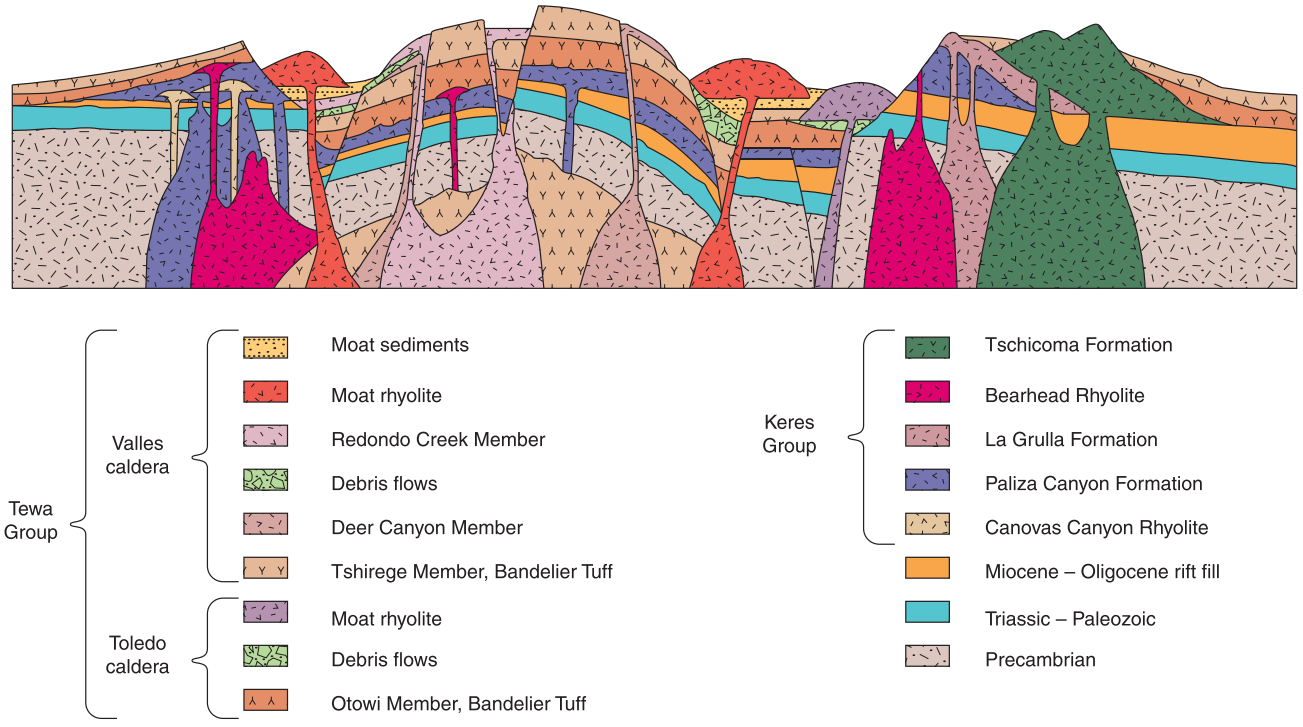

FIGURE 9—Conceptual model of the Valles caldera region showing the relative stratigraphic positions of the major volcanic units, the basic internal structure of the caldera, and the possible configuration of underlying magma chambers. The model is not necessarily to scale and has no specific orientation. More detailed cross sections may be found on the map sheet.

5. Differential resurgence of a highly fragmented caldera floor by rising Deer Canyon and Redondo Creek magmas resulting in many dike intrusions.
6. Uplifted debris-flow, fluvial, and lacustrine deposits on the resurgent dome.
7. Injection and eruption of magmas into the outer ring faults. It is compelling to think that the entire ring-fracture zone is filled with dikes, but there is presently no way to prove this.
8. Deposition of sediments and lacustrine rocks contemporaneous with ring-fracture volcanism.
9. Stratigraphy and temperature measurements obtained from many deep wells drilled to a maximum depth of 14,400 ft (4,390 m; EE-2). Although the wells were drilled primarily in and around the southwest quadrant of the caldera, they provide critical constraints on stratigraphy and temperature elsewhere. Temperature distributions for the northeast and eastern caldera region are derived from shallow well data interpreted by Sass and Morgan (1988).
10. A thick precaldera volcanic section beneath the upper Redondo Creek area. The volcanic rocks are identified as late Miocene Paliza Canyon Formation (primarily basalt and porphyritic andesite), but these rocks display intense hydrothermal alteration (Nielson and Hulen 1984; Hulen and Nielson 1986).
11. Localization of a high-temperature, convective geothermal system in the southwest quadrant of the caldera, particularly in the Redondo Creek graben and the faults near Sulphur Springs. Temperature isotherms around the west and south caldera margins are well constrained. Temperature isotherms east and northeast of the caldera may be slightly too high for a given depth.

Conceptual Valles Caldera Model

Figure 9 presents a conceptual model to visualize some important features of the Jemez Mountains volcanic field in the vicinity of Valles caldera. The model is not to scale, and the model does not present any specific orientation, although the left third of the diagram generally represents the southern flank of the caldera, the center third is oriented perpendicular to the Redondo Creek graben, and the right third represents the northeast flank of the caldera; depth of the model's section is around 3–4 mi (5–7 km). The units are presented more or less in descending stratigraphic position. Volcaniclastic sedimentary units such as the Puye and Cochiti Formations are omitted for clarity.

First, the model shows the relative stratigraphic positions of the major volcanic units in the Tewa and Keres Groups with respect to the Santa Fe Group and other rift fill rocks, Triassic to Mississippian sedimentary strata, and Precambrian basement. Second, the model shows the basic internal structure of the Valles caldera and the resurgent dome. Note that resurgence around the outer margin of the dome is mostly accommodated along high-angle, outward-dipping normal faults. We believe these faults were reactivated, inner ring, collapse faults as discussed above. Third, the model shows the hypothetical configuration of underlying magma bodies that fed the major volcanic units in the Jemez Mountains. The model

shows the now-recognized broader distribution of Bearhead Rhyolite and multiple magma bodies in the Bandelier composite stock beneath the Valles caldera.

Because Toledo caldera is largely obliterated by the later Valles caldera, no attempt is made to show the structural configuration of Toledo or its underlying magma body. Deep drilling has verified that collapse took place during formation of Toledo caldera, but drilling strongly suggests that structural resurgence did not take place after formation of Toledo. As a result, we have only shown a fragment of the Toledo ring-fracture zone and a moat rhyolite in the right-central part of the model.

Acknowledgments

The authors wish to thank the following geoscientists who participated in the mapping of the quadrangles used in this geologic compilation: Robert Osburn, Cathy J. Goff, Paul Drakos, Danny Katzman, Charles Ferguson, Scott Lynch, Michael Rampey, Magdalena Sandoval, Mary Osburn, Eric Trujillo, and Scott Kelley. Paul Drakos (*Glorieta Geoscience*), Richard Chamberlin, and Bruce Allen (both of the New Mexico Bureau of Geology and Mineral Resources (NMBGMR)) participated in a pre-production field review. The fabulous cartographic skills of Rebecca Titus Taylor (*Prisma Light Studio*) are gratefully appreciated as are the Arc/GIS-map database skills of Shannon Williams, Jennifer Whiteis, Mark Mansell, and Lewis Gillard (NMBGMR). Jane Love edited the map and text. Julie Hicks produced the final layout for the map and text. Funding was provided by STATEMAP (joint between the U.S. Geological Survey and the NMBGMR), the U.S. Forest Service, the Los Alamos National Laboratory, The National Park Service, and the Valles Caldera National Preserve. The authors would like to thank J. Michael Timmons, Paul Bauer (NMBGMR), Michael Linden (U.S. Forest Service), John Browne (LANL), Bruce Heise (NPS), Robert Parmenter, and Dennis Trujillo (both VCNP) for making this effort possible. Ana Steffen contributed important archaeological information to the text and rock descriptions. Detailed peer reviews were provided by David Broxton (LANL), John Stix (McGill University, Canada), and Richard Chamberlin (NMBGMR).

Description of Map Units

Note: Descriptions of map units are listed in approximate order of increasing age. Formal stratigraphic names are described in Griggs (1964), Bailey et al. (1969), and Smith et al. (1970) with usage revised in Gardner et al. (1986), Self et al. (1988), Goff and Gardner (2004), Kelley et al. (2007a), Gardner et al. (2010), Kelley et al., in press, and geologic maps shown in key. Names of volcanic rocks are based on phenocryst identification in hand specimens and petrographic examination of thin sections, and do not necessarily agree with geochemical classifications (Wolff et al. 2005; Rowe et al. 2007). Place names and physiographic features are shown in Figures 1, 2, and 3. Magnetic polarities from Doell et al. (1968) unless otherwise noted.

CENOZOIC

Holocene to Pleistocene fluvial, mass wasting, eolian, and spring deposits

Qdi — **Disturbed areas**–Anthropogenically disturbed areas consisting of underlying rock units at each site; not shown in correlation chart; maximum thickness less than 5 m

Qal — **Alluvium** (mostly Holocene)–Deposits of sand, gravel, and silt in main valley bottoms; maximum thickness may exceed 15 m

Qc — **Colluvium** (mostly Holocene)–Poorly sorted slope wash and mass wasting deposits from local sources; mapped only where extensive or where covering critical relations; thickness locally exceeds 15 m

Qaf, Qafu — **Alluvial fans** (late Holocene to late Pleistocene)–Typically fan-shaped deposits of coarse to fine gravel and sand, silt, and clay within and at the mouths of valleys and inside north and east caldera margins; some fan deposits (*Qafu*) are difficult to distinguish from older alluvial fans (described below); maximum exposed thickness about 15 m

Qes — **Wind-blown deposits** (Holocene)–Fine-grained, tan eolian silt on mesa tops; on Cat Mesa east of Cañon de San Diego, this unit consists of well-sorted, reddish-brown to brown wind-blown silt and fine-grained sand that overlies and is mixed with reworked, biotite-bearing pumice tentatively correlated with El Cajete Pyroclastic Bed pumice; varies in thickness from about 1 to 5 m

Qls — **Landslides** (late Holocene to late Pleistocene)–Poorly sorted debris that has moved chaotically down steep slopes; includes slumps or block slides that are partially to completely intact; thickness varies considerably depending on the size and nature of the landslide

Qrx — **Boulder fields** (Holocene to Pleistocene)–Areas covered with boulders as large as 3m derived from subjacent rock units; generally devoid of vegetation; many appear to be rock glaciers, exhibiting flowage features such as arcuate pressure ridges (Blagbrough 1994); thickness unknown

Qt — **Younger stream terraces** (inferred Holocene or late Pleistocene)–Deposits of sand, gravel, and silt that underlie young terrace surfaces bordering present streams; maximum thickness uncertain

Qts — **Sulphur Creek terraces** (Holocene to late Pleistocene)–Deposits of gravel, sand, silt, peat, and minor lacustrine beds along the edges of Sulphur Creek; maximum thickness probably 15 m

Qs — **Terrace sandstone** (Pleistocene)–Fine-grained, poorly consolidated, white sandstone of uncertain origin located 10–15 m above the present level of the Jemez River downstream of La Cueva; contains pumice lapilli; thickness about 2–3 m

Qto — **Older stream terraces** (late Pleistocene)–Deposits of sand, gravel, and silt that underlie higher terraces at various elevations and generally post-date lakes that occupied major valleys in the caldera; old terrace gravels along San Antonio Creek contain a variety of volcanic rocks ± rare Precambrian clasts ± Banco Bonito Flow rhyolite; terrace north of La Cueva is 29.0 ± 0.3 ka (Goff and Gardner 2004); typical thickness is 1–2 m but locally may exceed 10 m

Qlso — **Older landslides** (late Pleistocene)–Older slide deposits that are overlain by several types of younger deposits; may include **Qmso** in north caldera area; maximum exposed thickness about 25 m

Qtro — **Old travertine deposits** (Pleistocene)–Deposits of calcium carbonate from inactive springs ranging from porous tufa to banded travertine; unit locally contains white, finely bedded lake deposits less than 0.1 m thick; located on west wall of Cañon de San Diego; total thickness of unit is about 1–2 m

Qgbt — **Gravel deposit** (Pleistocene)–Gravel composed of scattered, rounded Bandelier Tuff clasts onlapping older Tertiary gravels (*QTgo*) and Paliza Canyon Formation andesite (*Tpa*) immediately south of La Cueva; likely derived from an ancestral San Antonio Creek; thickness is less than 1 m

Pleistocene intracaldera sedimentary and hydrothermal deposits

Qafo — **Older alluvial fans** (mainly Pleistocene)–Older deposits within Valles caldera consist of coarse to fine gravel and sand, silt, and clay derived mostly from the volcanic domes, resurgent dome, and caldera walls; deposits commonly post-date the lakes that occupied major valleys and have been incised. Alluvial fans west of Battleship Rock overlie old colluvium dominated by Paliza Canyon Formation andesite cobbles and contain rounded sandstone clasts derived from the Permian Abo Formation and Yeso Group. Various deposits are mainly Pleistocene in age although, typically, portions are still active; thickness is unknown

Qg3, Qg2, Qg1 — **Sedimentary deposits of southern caldera** (Pleistocene)–Alluvium, colluvium, debris flows, and minor lacustrine deposits interbedded with silicic lavas and pyroclastic rocks in the southern Valles caldera; formed during at least three episodes of incision and blockage of the ancestral East Fork Jemez River and tributaries. **Qg3** underlies the Banco Bonito Flow rhyolite (*Qvb*) but overlies El Cajete Pyroclastic Beds (*Qvec*) and Battleship Rock Ignimbrite (*Qvbr*); **Qg2** overlies South Mountain Member rhyolite (*Qvsm*) but underlies the El Cajete Pyroclastic Beds (*Qvec*) and Battleship Rock Ignimbrite (*Qvbr*); **Qg1** underlies the South Mountain Member rhyolite (*Qvsm*); maximum exposed thickness is about 40 m

Qlec / Qlb — **El Cajete lake deposits** (Pleistocene)—Deposits of reworked El Cajete Pyroclastic Beds and coarse sand in the Valle Grande (**Qlec**) that formed when pumice deposits dammed the East Fork Jemez River (Reneau et al. 2007); **Qlb** designates constructional landforms along and near the margin of the lake, including beach ridges and spits; age about 50–60 ka; maximum exposed thickness about 4 m

Qlsm — **South Mountain lake deposits** (Pleistocene)—Laminated to bedded, diatomaceous silty clay and mudstone; minor siltstone and sandstone; found in Valle Grande (Conover et al. 1963; Griggs 1964; Reneau et al. 2007; Fawcett et al. 2007, 2011); lake formed when South Mountain Member rhyolite dammed drainage of the East Fork Jemez River; possibly interbedded with older alluvial fan deposits (*Qafo*); age 552 to about 368 ka; maximum drilled thickness in Valle Grande is about 95 m

Ql — **Lacustrine deposits in northern caldera** (Pleistocene)—Finely laminated deposits of clay, silt, and very fine sand with subordinate fine to coarse sand and gravel; deposited in lakes that occupied Valle San Antonio, Valle Toledo, and Valle Santa Rosa; formed by blockage of drainages by post-resurgence eruptions from ring-fracture vents (Rogers et al. 1996; Reneau et al. 2007); deposits sometimes tuffaceous, and diatomaceous facies present; locally may contain fossil remains; locally silicified from hydrothermal alteration; age roughly 400 to >800 ka; maximum exposed thickness about 20 m

Qso — **Older intracaldera sandstone** (Pleistocene)—Weakly indurated to unconsolidated, moderate- to well-sorted, subrounded, medium-grained, reddish-tan quartz lithic sand with scattered pumice clasts; locally thinly crossbedded. Unit overlies northeast portions of Cerro Seco Member lava dome at 9,000 ft; maximum exposed thickness about 20 m

Qmso — **Older sedimentary deposits of northern caldera** (Pleistocene)—Debris-flow, landslide, and fluvial deposits that resemble early caldera-fill sediments (*Qdf*, described below) but include fragments of lava and pumice from Cerro del Medio Member rhyolites; age about 1.2–0.9 Ma; maximum exposed thickness about 25 m

Qvsc / Qvs — **Early caldera-fill lacustrine and fluvial deposits** (Pleistocene)—Laminated to thinly bedded, diatomaceous mudstone and siltstone, and crossbedded to normally graded sandstone and conglomerate; some beds contain ripple marks, flute casts, and plane laminations and may be deltaic deposits near margins of initial caldera lake; **Qvsc** consists of sandstone, siltstone, and lacustrine beds containing abundant biotite from weathering of Redondo Creek Member rhyodacite; beds generally display zeolitic or less commonly acid sulfate alteration (Chipera et al. 2007); beds generally deformed by uplift of resurgent dome; age is 1.25–1.1 (?) Ma; maximum exposed thickness about 30 m

Qdf — **Early caldera-fill debris-flow, landslide, alluvium, and colluvium deposits** (Pleistocene)—Matrix-supported conglomerates containing particles ranging in size from clay to boulders of various early postcaldera rhyolites, Bandelier Tuff, precaldera volcanic rocks, Miocene to Permian sandstone, Pennsylvanian limestone, and Precambrian crystalline rocks; finer-grained matrix is generally not exposed; contains minor fluvial sand and gravel deposits; lower part of unit displays extensive, low-grade hydrothermal alteration (Chipera et al. 2007); interbedded with and overlies all other units on resurgent dome; age is 1.25 to 1.0 (?) Ma; maximum exposed thickness is 70 m; maximum drilled thickness in Baca–7 well on northeast side of resurgent dome is more than 400 m (Lambert and Epstein 1980)

Qst — **Sinter deposits** (Pleistocene)—Small, widely scattered outcrops of massive to banded silica-rich hot spring deposits from early hydrothermal activity on resurgent dome; may contain Fe-oxides; may contain fossil reeds and other organic remains; maximum exposed thickness about 3 m

TEWA GROUP (Pleistocene)

Valles Rhyolite

East Fork Member

Qvb — **Banco Bonito Flow**—Thick rhyolite lava flows that contain phenocrysts of plagioclase, quartz, biotite, hornblende, clinopyroxene, and rare sanidine in a glassy to devitrified groundmass; upper surface of unit preserves pressure ridges and valleys with as much as 20 m of relief; fills paleovalleys in southern ring-fracture zone; unit dated at 34–45 ka (Ogoh et al. 1993; Phillips et al. 1997; Goff and Gardner 2004; Lepper and Goff 2007); magnetic polarity normal; maximum exposed thickness roughly 140 m

Qvcr — **VC-1 rhyolite**—(*Shown in cross section B–B′ only*) Flow-banded rhyolite lava containing sparse phenocrysts of plagioclase, quartz, biotite, clinopyroxene, hornblende, and rare sanidine in a glassy to perlitic groundmass; apparently fills shallow paleovalley in southern ring-fracture zone; found only in VC–1 core hole where it is 19 m thick (Gardner et al. 1987; Goff and Gardner 1994); magnetic polarity normal (Geissman 1988); age not resolved but probably around 50 ka

Qvbr — **Battleship Rock Ignimbrite**—Rhyolitic pyroclastic flows and surge deposits with lithic clasts; pumice contains phenocrysts of plagioclase, quartz, biotite, hornblende, clinopyroxene, and rare sanidine; smaller ignimbrites interbedded with the upper part of the El Cajete Pyroclastic Beds pumice; mostly fills paleocanyons in southwestern moat of Valles caldera; estimated age is 50–60 ka (Toyoda et al. 1995; Reneau et al. 1996); magnetic polarity normal; maximum exposed thickness about 60 m

Qvec — **El Cajete Pyroclastic Beds**—Moderately sorted beds of pyroclastic fall and thin pyroclastic flow deposits; rhyolite pumice clasts contain sparse phenocrysts of plagioclase, quartz, and biotite with rare microphenocrysts of hornblende and clinopyroxene; unit dated at about 50–60 ka (Toyoda et al. 1995; Reneau et al. 1996); magnetic polarity normal (Geissman 1988); maximum exposed thickness varies from 70 m in vent area to scant exposures too thin to map

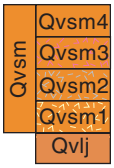

South Mountain Member–Flow-banded, massive to slightly vesicular porphyritic rhyolite lavas containing abundant phenocrysts of sanidine, plagioclase, quartz, biotite, hornblende, and clinopyroxene in a pale-gray, perlitic to white, devitrified groundmass; apparently consists of four flow units based on morphology (youngest to oldest **Qvsm4** to **Qvsm1**); fills paleocanyon in southern moat of Valles caldera; $^{40}Ar/^{39}Ar$ age of *Qvsm2* is 0.52 ± 0.01 Ma (Spell and Harrison 1993); maximum exposed thickness is at least 450 m. Includes Cerro La Jara rhyolite (**Qvlj**), a small dome of flow-banded, massive to slightly vesicular porphyritic lava; $^{40}Ar/^{39}Ar$ age is 0.53 ± 0.01 Ma (Spell and Harrison 1993); magnetic polarity normal; maximum exposed thickness about 75 m

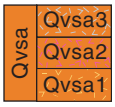

San Antonio Mountain Member–Flow-banded, massive to slightly vesicular rhyolite lavas containing phenocrysts of sanidine, plagioclase, quartz, biotite, hornblende, and clinopyroxene; consists of two main flow units based on morphology (**Qvsa2** and **Qvsa1**) erupted from San Antonio Mountain; a third flow and peripheral vent (**Qvsa3**) may be present at Sulphur Point; $^{40}Ar/^{39}Ar$ age of *Qvsa1* is 0.557 ± 0.004 Ma (Spell and Harrison 1993); magnetic polarity normal; maximum exposed thickness at least 510 m

Cerro Seco Member–Flow-banded, massive to slightly vesicular rhyolite lavas containing phenocrysts of quartz, sanidine, biotite, and rare hornblende; consists of two flow units based on morphology (**Qvse2** and **Qvse1**); $^{40}Ar/^{39}Ar$ age is 0.800 ± 0.007 Ma (Spell and Harrison 1993); magnetic polarity reverse; maximum exposed thickness is 375 m. Pyroclastic deposits (**Qvset**) consist of ignimbrite and dry surge near the vent, to probable hydromagmatic surge and derivative pumice-rich sediments distally; pumice lapilli have same mineralogy as flows; dates on pumice in ignimbrite and hydromagmatic deposit are 0.77 ± 0.03 and 0.78 ± 0.04 Ma, respectively (Kelley et al., in press); thickness of all pyroclastic deposits ranges from roughly 75 m at north edge of dome complex to < 1 m at distal sites

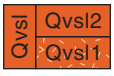

Cerro San Luis Member–Flow-banded, massive to slightly vesicular porphyritic rhyolite lavas containing phenocrysts of sanidine, quartz, and biotite; locally spherulitic; dome consists of two eruptive pulses based on morphology (**Qvsl2** and **Qvsl1**). $^{40}Ar/^{39}Ar$ age is 0.800 ± 0.003 Ma (Spell and Harrison 1993); magnetic polarity reverse; maximum exposed thickness is 325 m

Cerro Santa Rosa Member–Two temporally distinct, juxtaposed rhyolite domes that have the same name. **North dome** (**Qvsr2**) consists of massive to flow-banded porphyritic lava with quartz, subordinate sanidine, and trace biotite; dated by $^{40}Ar/^{39}Ar$ at 0.787 ± 0.015 Ma (Spell and Harrison 1993); magnetic polarity reverse; maximum thickness about 150 m. **South dome** (**Qvsr1**) consists of porphyritic lava with abundant quartz, subordinate sanidine, and sparse, small biotite; dome exhibits a breccia apron around summit; dated by $^{40}Ar/^{39}Ar$ at 0.914 ± 0.004 Ma (Spell and Harrison 1993) and 0.936 ± 0.008 Ma (Singer and Brown 2002); magnetic polarity transitional; maximum thickness more than 240 m. **Pyroclastic flow and fall deposits** (**Qvsrt**) consists of pumice lapilli with phenocrysts of quartz, sanidine, and biotite in a highly vesicular groundmass; fall deposits contain abundant lithic fragments; $^{40}Ar/^{39}Ar$ age on pumice in pyroclastic flow is 0.91 ± 0.03 Ma (Kelley et al., in press) and is therefore related to *Qvsr1* eruption; maximum thickness is about 25 m

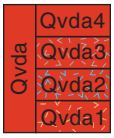

Cerros del Abrigo Member–Complex of four rhyolite dome and flow sequences: **devitrified lava** (**Qvda4**) with small phenocrysts of sanidine, subordinate quartz and plagioclase, and trace biotite and hornblende; maximum exposed thickness about 255 m; **devitrified lava** (**Qvda3**) with large phenocrysts of sanidine, lesser amounts of plagioclase, large but sparse quartz, sparse biotite, and rare hornblende; maximum exposed thickness about 245 m; **perlitic lava** (**Qvda2**) with phenocrysts of sanidine, subordinate plagioclase, sparse biotite and quartz, and trace hornblende; maximum exposed thickness about 405 m; apron of **perlitic, porphyritic lava** (**Qvda1**) exposed on erosional platforms around south side of dome complex; phenocrysts consist of sanidine, subordinate plagioclase and quartz, sparse biotite, and trace hornblende; maximum exposed thickness about 65 m. Composite $^{40}Ar/^{39}Ar$ age for the entire complex is 0.973 ± 0.010 Ma (Spell and Harrison 1993); magnetic polarity normal

Cerro del Medio Member–Rhyolite dome and flow complex consisting of at least six eruptive phases (Gardner et al. 2007): **pyroclastic flow and pumice-fall deposits** (**Qvdmt**); pumice is sparsely porphyritic with small sanidine and opaque oxides; unit is likely associated with summit eruption of *Qvdm6* based on mineral similarities; maximum thickness about 4 m; **massive, devitrified, vesicular lava** (**Qvdm6**) with sparse, small phenocrysts of sanidine and opaque oxides; maximum exposed thickness about 45 m; **upheaved dome of glassy to devitrified lava** (**Qvdm5**) with very sparse sanidine phenocrysts and extremely rare clinopyroxene and zircon; maximum exposed thickness about 215 m; **massive, aphyric obsidian flow** (**Qvdm4**) that is flow banded and devitrified around unit margins; $^{40}Ar/^{39}Ar$ age is 1.169 ± 0.005 Ma (E. Phillips, unpubl. data); exposed thickness about 260 m. The three oldest flow lobes do not permit discrimination of their sequence; thus, they are designated north, west, and south, respectively. **Vesicular, flow-banded, glassy to devitrified lava** (**Qvdmn**) with sparse phenocrysts of sanidine and rare clinopyroxene; maximum exposed thickness about 30 m. **Obsidian flow** (**Qvdmw**) is locally devitrified and flow banded; nearly aphyric with small sanidine and very sparse magnetite; maximum exposed thickness about 120 m; **flow-banded, sparsely porphyritic lava** (**Qvdms**) with phenocrysts of sanidine, hornblende, quartz, and rare plagioclase; $^{40}Ar/^{39}Ar$ age is 1.229 ± 0.017 Ma (Phillips et al. 2007); obsidian flows are source of many artifacts (Baugh and Nelson 1987; Steffen 2005); maximum exposed thickness about 75 m; magnetic polarity reverse

Redondo Creek Member–Massive to flow-banded, porphyritic rhyodacite lavas containing plagioclase, biotite, clinopyroxene, and sanidine phenocrysts in a perlitic to devitrified groundmass; commonly spherulitic; contains substantial flow breccia; only silicic lavas in Valles caldera that do not contain quartz; unit displays extensive hydrothermal alteration; $^{40}Ar/^{39}Ar$ ages of four domes and flows range from 1.24 to 1.21 Ma (Phillips et al. 2007); sediments are interbedded with the rhyodacite north of La Cueva; maximum exposed thickness is about 180 m

Qdc / Qdct — **Deer Canyon Member**–Rhyolitic lava flows and tuffs characterized by phenocrysts of sanidine and quartz; porphyritic lavas are present on southwestern resurgent dome, whereas aphyric lavas are on central and eastern resurgent dome; $^{40}Ar/^{39}Ar$ ages of three flows range from 1.28 to 1.25 Ma (Phillips et al. 2007); maximum exposed thickness about 40 m. Lithic- and crystal-rich, thin-bedded rhyolitic tuffs (**Qdct**) are interbedded with lavas; pumice fragments usually contain phenocrysts of quartz and sanidine; lithic fragments generally consist of Bandelier Tuff and precaldera volcanic rocks; finer beds locally contain accretionary lapilli and appear to be hydromagmatic surge in origin; $^{40}Ar/^{39}Ar$ ages of five tuffs range from 1.27 to 1.23 Ma (Phillips et al. 2007); all units are extensively altered to zeolites, silica, Fe-oxides, and clay (Chipera et al. 2007); maximum exposed thickness about 30 m

Pleistocene sedimentary rocks on the Tshirege Member, Bandelier Tuff

Qalo — **Older alluvium** (Pleistocene)–Gravel, sand, and silt generally overlying the Tshirege Member of the Bandelier Tuff on the rim and flanks of Valles caldera; largely pre-date incision of canyons in surrounding plateaus and highlands; gravels consist primarily of volcanic fragments from sources near the deposits and possibly from within the caldera; roughly contemporaneous in age to north caldera sediments (*Qmso*) and early caldera debris flows (*Qdf*); maximum exposed thickness about 6 m

Qrd2 — **Young Rabbit Mountain debris-flow deposits** (Pleistocene)–Two debris-flow deposits overlying the Tshirege Member of the Bandelier Tuff immediately south of Rabbit Mountain; general features resemble those of *Qrd1* (described below) except the matrix is not as ash rich; maximum exposed thickness is about 60 m

Bandelier Tuff (Upper)

Qbx — **Vent and/or hydrothermal breccia**–Widely scattered, lenticular to nearly circular outcrops of mosaic or vent breccia, commonly located near or along faults and less than 300 m in diameter; composed primarily of rounded to subrounded fragments of Bandelier Tuff (*Qbt*) in matrix of fine-grained tuff; may also contain abundant to rare fragments of precaldera rocks; may be hydrothermally altered; breccias of this type do not display gouge and shear fabric typical of fault breccia; thickness usually not measurable

Qbt — **Bandelier Tuff, Tshirege Member**–Multiple flows of densely welded to nonwelded rhyolitic ash-flow tuff erupted during formation of the Valles caldera (Smith and Bailey 1966, 1968); pumice and matrix contain abundant phenocrysts of sanidine and quartz, sparse microphenocrysts of clinopyroxene and orthopyroxene, and extremely rare microphenocrysts of fayalite (Warshaw and Smith 1988; Warren et al. 2007); in more welded portions, sanidine typically chatoyant (blue iridescence); contains accidental lithic fragments of older country rock; locally has a thin (<2 m) laminated, pumice-fall and surge deposit at base of unit (Tsankawi Pumice Bed) that contains roughly 1% of hornblende dacite pumice (Bailey et al. 1969); most recent $^{40}Ar/^{39}Ar$ age determination is 1.25 ± 0.01 Ma (Phillips et al. 2007); magnetic polarity reverse; maximum observed thickness within caldera more than 900 m

Qx: Qxg, Qxbo, Qxt, Qxpt, Qxp, Qxsf, Qxab, Qxr, Qxa, Qxm, Qxp-Ꞓ — **Caldera-collapse breccia**–Caldera-wall landslide breccias (megabreccias) that accumulated synchronously during caldera formation (Lipman 1976); incorporated in and interbedded with intracaldera, upper and lower members of the Bandelier Tuff (*Qbt* and *Qbo*) (Goff et al. 2007); unit consists of: 1. (**Qxg** *[shown in cross section A–A′ only]*) Virgin Mesa Member, Cerro Toledo Formation gravel and sand deposits interbedded between the two members of the Bandelier Tuff; 2. (**Qxbo**) silicified and brecciated Otowi Member of the Bandelier Tuff; 3. (**Qxt**) Tschicoma Formation rhyodacite, dacite, and coarse volcaniclastic Puye Formation materials; 4. (**Qxpt**) Paliza Canyon Formation dacite tuff; 5. (**Qxp**) Paliza Canyon Formation andesite and volcaniclastic materials; 6. (**Qxsf**) Santa Fe Group well-sorted Ojo Caliente Sandstone; 7. (**Qxab** *[Abiquiu Formation shown in cross section B–B′ only]*) Light-tan, thin-bedded volcaniclastic sandstone; 8. (**Qxr**) Ritito Formation non-indurated sandstone and conglomerate locally rich in Precambrian cobbles and pebbles; 9. (**Qxa**) Permian Abo Formation and Yeso Group sandstone, siltstone, and shale; 10. (**Qxm**) Pennsylvanian Madera Formation limestone, micrite, and shale; 11. (**Qxp-Ꞓ** *[shown in cross section B–B′ only]*) Precambrian crystalline rocks; breccia blocks generally show baking and/or disaggregation textures around margins if contacts with enclosing *Qbt* are preserved; **Qx** volcanic breccias are dated at 1.68–8.21 Ma (n = 3; Phillips 2004); maximum exposed thickness is highly variable

Cerro Toledo Formation

Qcpc — **Pueblo Canyon Member** (Pleistocene)–Colluvial deposit of reworked pumice and angular blocks of Otowi Member tuff in middle Frijoles Canyon; two thin deposits of primarily Tschicoma Formation-derived gravels in upper Frijoles Canyon and northwest of Rendija Peak; interbedded between the two upper members of the Bandelier Tuff; equivalent to the Cerro Toledo interval (Broxton and Reneau 1995); maximum thickness about 4 m

Qcvm — **Virgin Mesa Member** (Pleistocene)–Gravel and sand deposits interbedded between the two upper members of the Bandelier Tuff within or around the south and west margins and outer flanks of Valles caldera; consists primarily of precaldera volcanic rocks, Otowi Member of the Bandelier Tuff ± Valle Toledo Member rhyolite and Permian sandstone; equivalent to the intracaldera S3 sandstone of Nielson and Hulen (1984); equivalent in time to the Cerro Toledo interval (Broxton and Reneau 1995) but has no Valle Toledo Member pumice; maximum exposed thickness is 15 m

Valle Toledo Member

Toledo embayment domes

Qcrt — **Rhyolite tuff**–Two areas of partially to densely welded, nearly aphyric tuff; microphenocrysts consist of sparse quartz, sanidine, biotite, and rare clinopyroxene; K–Ar age of west exposure (Pinnacle Peak) is 1.20 ± 0.02 Ma (Stix et al. 1988); maximum exposed thickness is roughly 200 m

Qcr **Aphyric rhyolite**–Two dome and flow complexes and two small intrusive bodies of flow-banded lava; obsidian phases are completely aphyric and probable source of artifacts (Steffen 2005); devitrified phases contain spherulites and very sparse microphenocrysts of quartz, sanidine, and biotite; K–Ar age of dome northwest of Cerro Rubio (*Tlcr*) is 1.33 ± 0.02 Ma (Stix et al. 1988); maximum exposed thickness is 365 m

Qcs **Sierra de Toledo rhyolite**–Flow-banded, sparsely porphyritic lava with phenocrysts of quartz, sanidine, biotite, and tiny magnetite; sanidine is typically chatoyant blue; possibly originates from two vents; $^{40}Ar/^{39}Ar$ ages of two samples range from 1.34 to 1.38 Ma (Spell et al. 1996); maximum exposed thickness is 365 m

Qctr **Turkey Ridge rhyolite**–Flow-banded, porphyritic lava with phenocrysts of quartz, sanidine, biotite, and magnetite; sanidine is commonly large and chatoyant; most samples are devitrified, platy, and spherulitic; has one vent along axis of ridge; $^{40}Ar/^{39}Ar$ age is 1.34 ± 0.02 Ma (Spell et al. 1996); maximum exposed thickness is 490 m

Qct **Cerro Toledo rhyolite**–Flow-banded, aphyric lava with microlites of quartz, sanidine, biotite; obsidian phase is completely aphyric and known source of artifacts (Steffen 2005); rarely contains spherulites and bread crust textures; overlies Indian Point rhyolite (*Qci*) and apparently underlies Turkey Ridge rhyolite (*Qctr*); underlies Tshirege Member of the Bandelier Tuff (*Qbt*); originates from two vents; K–Ar age on Cerro Toledo proper is 1.38 ± 0.05 Ma (Stix et al. 1988); maximum exposed thickness is 520 m

Qci **Indian Point rhyolite**–Flow-banded, sparsely porphyritic lava with phenocrysts of quartz and sanidine; biotite is extremely rare; most samples are devitrified and spherulitic; $^{40}Ar/^{39}Ar$ age is 1.46 ± 0.01 Ma (Spell et al. 1996); maximum exposed thickness is 410 m

Qcnr **North caldera rim intrusion**–Flow-banded, sparsely porphyritic intrusive body and minor lava having phenocrysts of quartz, sanidine, and biotite; $^{40}Ar/^{39}Ar$ age is 1.61 ± 0.03 Ma (Kelley et al., in press); maximum exposed thickness is 50 m

TOLEDO CALDERA RING-FRACTURE DOMES

Qcws **Warm Springs rhyolite**–Small dome of massive to flow-banded, porphyritic lava containing phenocrysts of quartz, sanidine, and biotite; $^{40}Ar/^{39}Ar$ age is 1.26 ± 0.01 Ma (Spell et al. 1996); maximum exposed thickness is 25 m

Qctq **Cerro Trasquilar rhyolite**–Flow-banded to massive, sparsely porphyritic lava with tiny phenocrysts of quartz, sanidine, clinopyroxene, opaque oxides, and rare biotite; erupted from a single vent; $^{40}Ar/^{39}Ar$ age is 1.36 ± 0.01 Ma (Spell et al. 1996); maximum exposed thickness 225 m

Qrd1 **Old Rabbit Mountain debris-flow deposits**–Debris flows formed by multiple failures of the Rabbit Mountain dome during growth; outcrops display sintered ashy matrix suggesting formation as glowing avalanches; contains abundant obsidian blocks that are a known source of artifacts (Steffen 2005); forms southeast-trending hummocky tongue 5 km long and 3 km wide between the two upper members of the Bandelier Tuff; maximum exposed thickness about 40 m

Qcrm / Qcrmt **Rabbit Mountain rhyolite**–Large dome with thick flows and flow breccias of aphyric to sparsely porphyritic obsidian to white, devitrified lava; obsidian is a known source of artifacts (Steffen 2005); actual vent area is probably northwest of location shown on map; vent collapsed before or during formation of Valles caldera; small exposure of associated bedded tuff (**Qcrmt**) is southwest of dome; $^{40}Ar/^{39}Ar$ age is 1.428 ± 0.007 Ma (Kelley et al., in press); maximum exposed thickness about 410 m

Qcep **East Los Posos rhyolite**–Flow-banded to massive porphyritic lava with phenocrysts of quartz, sanidine, biotite, hornblende, opaque oxides; rarely contains black glassy groundmass; $^{40}Ar/^{39}Ar$ age is 1.45 ± 0.01 Ma (Spell et al. 1996); maximum exposed thickness 165 m

Qnd **Paso del Norte debris avalanche deposit**–Debris flows apparently formed by failure of Paso del Norte dome; forms irregular tongue of chaotic debris extending 4 km south–southeast; present between the Tshirege and Otowi Members of the Bandelier Tuff; maximum exposed thickness about 60 m

Qcnp / Qcnpt **Paso del Norte rhyolite**–Small dome and flow of devitrified rhyolite with sparse phenocrysts of quartz, sanidine, and biotite; layer of indurated, slightly altered, lithic-rich tuff (**Qcnpt**) underlies dome on east and southeast; $^{40}Ar/^{39}Ar$ age is 1.47 ± 0.04 Ma (Justet and Spell 2001); maximum exposed thickness about 110 m

Qcwp **West Los Posos rhyolite**–Flow-banded to massive porphyritic rhyolite with phenocrysts of quartz, sanidine, plagioclase, biotite, and opaque oxides; commonly contains relict black glass; $^{40}Ar/^{39}Ar$ age is 1.54 ± 0.01 Ma (Spell et al. 1996); maximum exposed thickness 370 m

BANDELIER TUFF (LOWER)

Qbo **Bandelier Tuff, Otowi Member**–Poorly to densely welded rhyolitic ash-flow tuff; originated from catastrophic eruptions that formed Toledo caldera; pumice and matrix contain abundant phenocrysts of sanidine and quartz, and sparse mafic microphenocrysts; sanidine may display a blue iridescence; contains abundant accidental lithic fragments; basal Guaje Pumice Bed to east described by Bailey et al. (1969) not found in map area; $^{40}Ar/^{39}Ar$ ages 1.61 ± 0.01 to 1.62 ± 0.04 Ma (Izett and Obradovich 1994; Spell et al. 1996); magnetic polarity reverse; maximum exposed thickness about 120 m

Qgo **Older gravels** (Pleistocene)–Fluvial sandstone and gravel deposited beneath the Otowi Member or between the Otowi and La Cueva Members of the Bandelier Tuff; gravel clasts composed predominantly of Paliza Canyon volcanic rocks with local Proterozoic granite, Permian sandstone and conglomerate, and rare Oligocene to Miocene Pedernal chert; maximum thickness 7 m

Qblc **Bandelier Tuff, La Cueva Member**–Nonwelded to poorly welded ash-flow tuff containing phenocrysts of quartz and sanidine with trace pyroxene and magnetite; consists of two units (Self et al. 1986; Spell et al. 1990); **upper unit** is nonwelded to slightly welded and contains large pumice clasts; **lower unit** is nonwelded and includes abundant lithic fragments. The two units are separated by reworked pumice and debris flows; $^{40}Ar/^{39}Ar$ ages are 1.85 ± 0.07 and 1.85 ± 0.04 Ma for the upper and lower units, respectively (Spell et al. 1996); previously called San Diego Canyon ignimbrites (Self et al. 1986); maximum observed thickness is 80 m

QUATERNARY–TERTIARY

QTg **Old fluvial gravel** (early Quaternary to late Pliocene?)–Single deposit of gravel composed of Permian sedimentary rocks and precaldera volcanic rocks high (~ 300 m) above the east side of Jemez River south of Battleship Rock on Cerro Colorado; overlies Permian so exact age is difficult to assess; maximum thickness 3 m

QTgo **Older fluvial gravels**–Conglomerate and sandstone that underlie the La Cueva Member, Bandelier Tuff; composed primarily of precaldera volcanic rock with local granite, sandstone, conglomerates, and rare Pedernal chert supported in a silt- to sand-sized matrix; locally pumiceous; probably correlate in time with Cochiti Formation (Smith and Lavine 1996); maximum thickness 12 m

QTp **Puye Formation**–Thin deposit of poorly exposed gravel above north wall of upper Quemazon Canyon; poorly exposed layer of gravel beneath **Qbo** in upper Frijoles Canyon; composed almost entirely of dacitic materials shed from the Tschicoma Formation; bracketed between about 2 and 5 Ma (Goff and Gardner 2004); maximum thickness about 15 m

QTl **Lake deposits**–Diatomaceous (?) fine-grained sandstone locally sitting on debris avalanche deposits (*Tls*, described below) north of Rincon Negro in Cañon de San Diego; the margins of the deposit are silicified, preserving finely laminated, alternating light and dark layers; maximum thickness 5 m

TERTIARY (Pliocene–Oligocene)

Tls / Tdf **Debris avalanche and debris-flow deposits**–Multiple block and ash flows (?) and/or volcanic landslides (**Tls**) with fragments consisting primarily of porphyritic andesite and basaltic andesite, locally in an ashy matrix. These deposits overlie a debris flow (**Tdf**) dominated by clasts of Abiquiu Formation sandstone, Paliza Canyon Formation andesite, and Tschicoma Formation (?) dacite just south of Agua Durme Springs; maximum thickness on Rincon Negro is 180 m

Tct **Block of tuff**–Block of a white pyroclastic flow containing clasts of devitrified rhyolite incorporated into andesitic debris avalanche (*Tls*, described above); may be part of Canovas Canyon Rhyolite tuff of Smith et al. (1970); the block is overlain by a brown, andesitic lapilli tuff and a fine-grained, flow-banded andesite flow; basal contact not exposed; minimum thickness about 10 m

Ts **Tertiary sediments, undivided** (Pliocene to Miocene?)–Two packages of red to tan, poorly exposed sedimentary units present along the western wall of Valles caldera; **upper unit** characterized by pebble- to cobble-sized angular pieces of Abiquiu Formation sandstone and Pedernal chert. **Lower unit** is a mix of rounded Tschicoma Formation dacitic and Paliza Canyon Formation volcanic clasts with local Abiquiu Formation sandstone in a sandy matrix. The latter is possibly reworked Ojo Caliente Sandstone Member (*Tsto*), described below; maximum thickness 70 m

KERES GROUP (Pliocene–Miocene)

TSCHICOMA FORMATION (Pliocene)

Ttqc **Upper Quemazon Canyon dacite**–Flow-banded to massive, slightly porphyritic lava with sparse phenocrysts of large plagioclase and small resorbed quartz in a trachytic groundmass of plagioclase, orthopyroxene, clinopyroxene, biotite, and opaque oxides; $^{40}Ar/^{39}Ar$ age is 2.92 ± 0.05 Ma (Kelley et al., in press); maximum exposed thickness is roughly 65 m

Ttpm **Pajarito Mountain dacite**–Dome and flow complex of massive to sheeted, porphyritic lava containing phenocrysts of plagioclase, hypersthene, clinopyroxene, and opaque oxides in a devitrified groundmass; $^{40}Ar/^{39}Ar$ ages on geographically separated samples range from 2.93 to 3.09 Ma (Broxton et al. 2007); maximum exposed thickness is about 365 m

Ttcb **Caballo Mountain dacite**–Dome and flow complex of massive to sheeted, porphyritic lava containing phenocrysts of plagioclase, oxidized hornblende, clinopyroxene, rare rounded quartz, opaque oxides, and oxidized biotite; $^{40}Ar/^{39}Ar$ age is 3.06 ± 0.15 Ma (Broxton et al. 2007); maximum exposed thickness is about 200 m

Ttcg **Cerro Grande dacite**–Extensive dome and flow complex of massive to sheeted, porphyritic lava containing phenocrysts of plagioclase, hypersthene, and (typically) conspicuous hornblende; the latter two phases commonly show oxidized rims that may be difficult to see in hand sample; ages on widely separated samples range from 2.88 to 3.35 Ma (Broxton et al. 2007); maximum exposed thickness is about 750 m

Ttsd **Sawyer Dome dacite**–Dome and flow complex of massive, porphyritic lava containing phenocrysts of plagioclase, hypersthene, opaque oxides, and conspicuous hornblende; contains local mafic clots of plagioclase-hornblende as large as 10 cm in diameter; $^{40}Ar/^{39}Ar$ age of summit is 3.44 ± 0.30 Ma (Kelley et al., in press); maximum exposed thickness is 245 m

Ttcr **Cerro Rubio dacite**–Massive to sheeted, fine-grained intrusive lava with phenocrysts of plagioclase, hornblende, orthopyroxene, biotite, and rare quartz; resembles *Ttcd* (described below); K–Ar age is 3.56 ± 0.36 Ma (Stix et al. 1988); maximum exposed thickness is 440 m

Ttcd **Dacite intrusion north of Cerro Rubio**–Massive to sheeted, fine-grained lava with small phenocrysts of plagioclase, hornblende, orthopyroxene, sparse biotite, and rare quartz; some columnar jointing visible around margins and top; $^{40}Ar/^{39}Ar$ age is 4.21 ± 0.12 Ma (Kelley et al., in press); maximum exposed thickness is 365 m

Ttsc **Santa Clara Canyon dacite**–Faulted, plug-like body of massive to sheeted, porphyritic lava containing phenocrysts of plagioclase, sanidine, hornblende, biotite, and sparse quartz; resembles dacite on and near Cerro Rubio; unit not dated; maximum exposed thickness is 160 m

Ttpd **Tschicoma Peak area dacite and rhyodacite, undivided**–Massive to sheeted, coarse porphyritic lavas having abundant phenocrysts of plagioclase and variable phenocrysts of biotite, hornblende, and rare clinopyroxene; younger lavas may contain phenocrysts of sanidine and quartz and 2–25-cm, elliptically shaped inclusions of mafic composition; $^{40}Ar/^{39}Ar$ ages are 3.57–4.46 Ma (Kempter et al. 2007); maximum exposed thickness >500 m

Ttrc **Rendija Canyon rhyodacite**–Dome and flow complex of massive to sheeted, highly porphyritic lavas with phenocrysts of quartz, sanidine, plagioclase, hornblende, and biotite; $^{40}Ar/^{39}Ar$ ages on widely separated samples range from 3.50 to 5.36 Ma (Broxton et al. 2007; Kelley et al., in press); maximum exposed thickness approximately 500 m

Ttd **Porphyritic dacite, undivided**–Massive to sheeted, porphyritic lava near Fenton Hill containing abundant phenocrysts of plagioclase and phenocrysts of biotite and hornblende; $^{40}Ar/^{39}Ar$ age is 4.36 ± 0.18 Ma (Kelley et al., in press); $^{40}Ar/^{39}Ar$ age on lava erupted from dome northwest of Tschicoma Peak is 5.34 ± 0.36 Ma (Kempter et al. 2007); maximum exposed thickness is 100 m

Ttu **Dacite and andesite, undivided**–(*Shown in cross section A–A′ only*) Porphyritic lava with phenocrysts of plagioclase, orthopyroxene, clinopyroxene ± quartz ± hornblende ± biotite; age bracketed between 2 and 5.5 Ma (Kempter et al. 2007); thickness in cross sections is speculative

Bearhead Rhyolite (Pliocene–Miocene)

Tbh **Bearhead Rhyolite**–Dikes, plugs, and flows of aphyric to slightly porphyritic, devitrified to completely silicified rhyolite containing sparse phenocrysts of quartz, sanidine, plagioclase, biotite, opaque oxides ± hornblende; locally shows pervasive hydrothermal alteration consisting of quartz, chalcedony and/or opal, illite, Fe- and Mn-oxides, pyrite, and possibly other sulfides, alunite, jarosite, and gypsum; $^{40}Ar/^{39}Ar$ ages on widely separated samples range from 4.81 to 7.83 Ma (Justet and Spell 2001; Kempter et al. 2007; Kelley et al., in press) maximum observed thickness about 100 m

La Grulla Formation (Miocene)

Tgbhd **Porphyritic biotite, hornblende rhyodacite**–Massive to sheeted, extremely porphyritic lava on north caldera rim having phenocrysts of sanidine, plagioclase, resorbed quartz, biotite, hornblende, clinopyroxene, orthopyroxene, and opaque oxides; contains rare iddingsitized olivine crystals and plagioclase-pyroxene-biotite clots; displays local hydrothermal alteration to silica, clay, chlorite, and Fe-oxides; $^{40}Ar/^{39}Ar$ age is 7.42 ± 0.05 Ma (Kelley et al., in press); maximum exposed thickness about 135 m

Tghd **Hornblende dacite and rhyodacite**–Massive to sheeted, porphyritic lavas of diverse texture capping Cerro de la Garita and other hills; flows have distinctive hornblende, plus plagioclase, sanidine, biotite, and minor clinopyroxene phenocrysts; erupted from several vents on southeastern La Grulla Plateau; $^{40}Ar/^{39}Ar$ ages range from 7.27 to 7.63 Ma (Kempter et al. 2007; Kelley et al., in press); maximum exposed thickness is 30 m

Tga **Porphyritic andesite and dacite, undivided**–Massive to sheeted, porphyritic lavas with phenocrysts of plagioclase, biotite, clinopyroxene, orthopyroxene, and opaque oxides; may contain plagioclase-pyroxene-biotite clots; erupted from multiple vents; $^{40}Ar/^{39}Ar$ ages on widely separated samples range from 7.43 to 7.81 Ma (Justet 2003; Kempter et al. 2007; Kelley et al., in press); maximum exposed thickness is about 330 m on north caldera wall

Tgb **Olivine basalt**–Two exposures of massive lava on northwestern caldera rim informally correlated with the basalt of Encino Point (Kelley et al. 2007a; Lawrence 2007); contain small phenocrysts of olivine, plagioclase, and clinopyroxene; interlayered with La Grulla Plateau andesite; $^{40}Ar/^{39}Ar$ ages are 7.80 ± 0.13 Ma (lower basalt) and 7.79 ± 0.09 Ma (upper basalt, Kelley et al., in press); maximum exposed thickness is roughly 35 m

Paliza Canyon Formation (Miocene)

Tpv / Tpvs **Volcaniclastic member** (Pliocene? to Miocene)–**Tpv** is conglomeratic sandstone and sandy conglomerate locally containing cinder deposits, pyroclastic- fall deposits, and lava flows too small or thin to map; unit has accumulated in small basins, topographic lows, and paleocanyons; contemporaneous with eruption of lavas of the Paliza Canyon Formation; upper part of unit may be correlative with oldest Cochiti Formation (Smith and Lavine 1996); maximum exposed thickness about 70 m. **Tpvs** is a moderately to well-sorted volcaniclastic sandstone that is brick red to tan and contains mostly volcanic fragments, feldspar, mafic minerals, and minor quartz; present between lava flow contacts in isolated locations throughout southeastern part of the map area; mapped only where laterally extensive and at least 3 m thick

Thb **Hydrothermal breccia**–Small areas in southeastern map area associated with volcanism of the Paliza Canyon Formation; consists of relatively circular, vertical pipes of mosaic breccia ≤ 100 m in diameter containing fragments of altered andesite and dacite in a fine-grained, silicified matrix; exact age unknown but probably ≤ 8 Ma (WoldeGabriel and Goff 1989); thickness is unknown

Tpd **Aphyric dacite**–Flow-banded to massive lavas containing sparse phenocrysts of plagioclase, pyroxene, hornblende, opaque oxides, and possibly potassium feldspar; plug-like body exposed north-northeast of Las Conchas is pervasively altered to chlorite, silica, and clay; intrusive breccia on the margins of the plug include small blocks and fragments of basalt and andesite in dacite host; ages of various units unknown; maximum exposed thickness about 120 m

Tpbd **Porphyritic biotite dacite**–Domes and flows having phenocrysts of plagioclase, biotite, and pyroxene; contains minor clots of plagioclase and pyroxene; commonly altered to silica, chlorite, clay, Fe-oxides, and minor calcite; $^{40}Ar/^{39}Ar$ ages on widely separated samples range from 7.38 to 7.78 Ma (Kelley et al., in press); maximum exposed thickness is 160 m

Tpdt **Porphyritic dacite tuff**–Distinctive unit of massive, lithic-rich tuff with conspicuous crystals of biotite and tiny hornblende, and crystals of plagioclase; contains lithic fragments of andesite, dacite, rhyolite, possible intrusive rocks, and sandstone in altered matrix of dense to vesicular tuff; alteration consists of silica, clay, Fe-oxides, and chlorite; exposed only in lower part of north caldera wall; K-Ar date of altered tuff is 8.20 ± 0.29 Ma (WoldeGabriel 1990); may be correlative with similar looking dacite tuff found as megabreccia block in northern part of resurgent dome (*Qxpt*), which has an $^{40}Ar/^{39}Ar$ age of 8.21 ± 0.08 Ma (Phillips 2004); maximum exposed thickness about 40 m

Tphd **Porphyritic hornblende dacite**–Eroded flows capping the summits of Las Conchas, Los Griegos, and other hills south of the caldera; phenocrysts consist of plagioclase, hornblende, orthopyroxene, and clinopyroxene; flows may contain plagioclase–pyroxene clots; some units pervasively altered to silica, Fe-oxides, calcite, and chlorite; $^{40}Ar/^{39}Ar$ age on Los Griegos is 8.53 ± 0.63 Ma (Kelley et al., in press); maximum exposed thickness is 75 m

Tpbhd **Porphyritic biotite, hornblende dacite**–Extensive dome and flow complex filling paleocanyon south of Rabbit Mountain; contains large phenocrysts of plagioclase, plus biotite, hornblende, orthopyroxene, and clinopyroxene; contains vesiculated enclaves of plagioclase, pyroxene ± hornblende ± biotite as large as 30 cm in diameter; hydrothermally altered to clay, silica, calcite, Fe-oxides, chlorite ± epidote; $^{40}Ar/^{39}Ar$ age is 8.66 ± 0.22 Ma (Kelley et al., in press); exposed thickness at least 275 m

Tpha **Hornblende andesite**–Plug of flow-banded, devitrified lava on southeast caldera margin having small phenocrysts of plagioclase, hornblende, clinopyroxene, and hypersthene; age of unit unknown; maximum exposed thickness about 45 m

Tppa **Porphyritic andesite**–Massive to sheeted flows of coarsely porphyritic lava having large phenocrysts of plagioclase and abundant phenocrysts of clinopyroxene and hypersthene; may contain plagioclase–pyroxene clots; flows in map area not dated; K–Ar age of similar flow at summit of St. Peter's Dome just east of map area is 8.69 ± 0.38 Ma (Goff et al. 1990); maximum observed thickness is about 150 m

Tpoa **Olivine andesite**–Dome and flow complex exposed in southeast map area; consists of massive to sheeted, slightly porphyritic lava with phenocrysts of plagioclase, clinopyroxene, olivine ± hypersthene; contains sparse plagioclase–pyroxene clots; age of unit unknown; maximum observed thickness about 70 m

Tpa **Two-pyroxene andesite, undivided**–Domes, flows, flow breccia, spatter deposits, and scoria of andesite from multiple sources; vents are widely scattered; individual units are slightly porphyritic to very porphyritic containing phenocrysts of plagioclase, orthopyroxene, and clinopyroxene; alteration varies from slight to intense consisting of silica, calcite, Fe-oxides, clay ± chlorite ± zeolite ± pyrite ± epidote; $^{40}Ar/^{39}Ar$ ages in western and southern map area range from 8.2 to 9.4 Ma (Justet 2003; Kelley et al., in press); maximum exposed thickness about 150 m

Tpb **Olivine basalt and basaltic andesite, undivided**–Flows, flow breccia, spatter deposits, and scoria of basalt and subordinate basaltic andesite from multiple vents; most units are slightly porphyritic containing phenocrysts of olivine, plagioclase ± clinopyroxene; displays variable amounts of hydrothermal alteration consisting of silica, calcite, Fe-oxides, clay ± zeolite ± chlorite ± epidote ± pyrite; $^{40}Ar/^{39}Ar$ ages from western and southern map areas range from 8.88 to 9.45 Ma (Justet 2003; Kelley et al., in press); maximum exposed thickness about 150 m

Bland intrusive rocks

Tm **Bland monzonite** (Miocene)–Dikes and plug of crystalline rocks in southeastern map area south of Evans-Griffin Place (see Bundy 1958; Stein 1983); textures range from coarse grained, hypidiomorphic granular, and seriate to fine grained, trachytic, and porphyritic; primary minerals consist of plagioclase, clinopyroxene, orthopyroxene, potassium feldspar, and sparse quartz ± biotite ± hornblende. Alteration is moderate to intense, argillic to propylitic; replacement minerals consist mainly of clays, Fe- and Mn-oxides, silica, calcite, illite, chlorite, epidote, and pyrite; widths of single dikes shown on map are usually exaggerated; vent area shown on map represents crystallized core of Paliza Canyon Formation volcano; crosscutting relations indicate age ≤9.5 Ma; K–Ar age on relatively unaltered sample from unspecified location in the Bland district southeast of map is 11.3 ± 0.3 Ma (Stein 1983); altered monzonite from stock in Bland district has $^{40}Ar/^{39}Ar$ ages ranging from 6.5 to 7.8 Ma (Kelley et al., in press); maximum exposed thickness is about 275 m

Canovas Canyon Rhyolite

Tcc **Canovas Canyon Rhyolite** (Miocene)–Hydrothermally altered lava in bottom of Medio Dia Canyon at Evans–Griffin Place; unit contains quartz, feldspar, biotite, and possibly hornblende altered to silica, clay, Fe-oxide, illite, and chlorite; some specimens contain calcite; underlies basalt; bottom of unit not exposed; age unknown but probably around 10 Ma; maximum exposed thickness about 10 m

Santa Fe Group

Tsf **Santa Fe Group, undivided** (Miocene)–Sandstone, siltstone, and conglomerate; relations with underlying Abiquiu Formation unclear; age roughly bracketed between 10 and 20 Ma; maximum observed thickness immediately southeast of map area is roughly 60 m; unit in VC–2B core hole is possibly Ojo Caliente Sandstone and is 48 m thick (Goff and Gardner 1994); unit in Redondo Creek geothermal wells as much as 262 m thick (Nielson and Hulen 1984)

Chamita Formation of the Santa Fe Group

Tscu **Hernandez Member (?)**–(Miocene) Thick sequence of sedimentary deposits dominated by arkosic sandstone but containing interbeds of pebbly conglomerate, debris flows, and breccias with subangular clasts of intermediate-composition volcanic rocks (Gardner and Goff 1996); locally altered to silica, iron oxides, clays, and chlorite; may be equivalent to the Hernandez Member of the Chamita Formation as implied by temporal constraints; age bracketed between 7.4 and 8 Ma; maximum thickness >200 m

Tesuque Formation of the Santa Fe Group

Tsto **Ojo Caliente Sandstone Member** (Miocene)–Poorly cemented, fine- to medium-grained sandstone consisting of subrounded to angular grains of quartz, feldspar, mafic minerals, and rare lithic fragments; high-angle crossbeds are locally preserved; age between about 12 and15 Ma; maximum thickness 10 m

Early Rio Grande rift sedimentary deposits

Tpc **Pedernal chert** (Miocene to Oligocene)–White to varicolored chert that is present as stringers or beds within the Abiquiu Formation and Ritito Conglomerate. This replacement deposit is as much as 5 m thick in this area

Ta **Abiquiu Formation** (Miocene to Oligocene)–White to tan, medium-grained, medium-bedded, volcaniclastic sandstone that is alternately well cemented and poorly cemented. Contains white, fine-grained ash beds that are <0.3 m thick and rare thin red mudstone intervals; maximum thickness 40 m

Tr **Ritito Conglomerate** (Miocene to Oligocene)–Weakly indurated arkosic fluvial conglomeratic sandstone with abundant pebble-sized Proterozoic granite, quartzite, and schist clasts, and few Pennsylvanian limestone and Permian sandstone clasts; maximum thickness 10 m

MESOZOIC

TRIASSIC

Ŧcu **Upper Chinle Group, undivided**–Includes the Salitral Shale, Poleo Sandstone, and Petrified Forest Formation. Primarily brick-red to maroon, poorly exposed mudstone; thin (<5 m) bed of black conglomerate with well-rounded chert and quartz pebbles belonging to the Poleo Sandstone is exposed south of East Fork Jemez River; estimated thickness 30 m

Ŧcs **Shinarump Formation, Chinle Group**–White to yellowish-brown, medium- to coarse-grained quartzose sandstone and conglomerate; conglomerate contains well-rounded chert, quartz pebbles, and petrified wood; sandstone typically cross-stratified, commonly in trough geometries; maximum thickness 20 m

Ŧm **Moenkopi Formation**–Reddish-brown, micaceous shale, silty shale, and crossbedded arkosic sandstone; unit is shale-rich at the base and sandy at the top; approximately 20 m thick

PALEOZOIC

PERMIAN

Pg — **Glorieta Sandstone**–White to gray, massive to planar-bedded to cross-stratified quartz arenite; typically well sorted; contact with the underlying Yeso Group is gradational; approximately 20 m thick

Py — **Yeso Group**–Red-orange to red, fine- to medium-grained quartzose sandstone; includes two formations in this region: the lower De Chelly (formerly Mesita Blanca) and the upper San Ysidro. The De Chelly Formation is well-sorted, eolian sandstone with meter-scale crossbeds. The San Ysidro Formation is medium-bedded, tabular sandstone that is orange red near the base and red near the top. A discontinuous 1–2-m-thick limestone bed is present near the top of the unit; maximum thickness 170 m

Pa — **Abo Formation**–Brick-red to dark-red, medium- and thin-bedded, arkosic, cross-stratified, fluvial sandstone; interbedded with micaceous siltstone and mudstone. The basal portion of the Abo Formation is dominated by mudstones; channel sands become thicker and more abundant in the upper part of the formation. Thin pedogenic carbonate beds are common on and just south of Cerro Colorado; maximum thickness about 260 m on Cerro Colorado

Pu — **Permian rocks, undivided**–(*Shown in cross sections only*) Combination of Yeso Group and Abo Formation; Glorieta Sandstone not identified beneath Valles caldera; commonly indurated in geothermal wells displaying considerable hydrothermal alteration and minor calcite and quartz veining; contact of Pu with underlying Madera Group is sharp to gradational depending on location; thickness is 90 m in VC–1 and 498 m in VC–2B core holes (Goff and Gardner 1994); thickness is 501 m in Baca–12 well (Nielson and Hulen 1984)

PENNSYLVANIAN–MISSISSIPPIAN

IPm — **Madera Group** (Pennsylvanian)–Light- to dark-gray, fossiliferous limestone, quartzose sandstone, arkose, arkosic limestone, and shale. The upper part of the unit grades into Abo Formation red beds and includes red arkosic sandstone and minor shale. The top was mapped at the uppermost limestone bed that is about 1 m thick. The upper 170 m of the unit is exposed in northern Cañon de San Diego

MIPu — **Pennsylvanian–Mississippian rocks, undivided**–(Shown in cross sections only.) This subsurface unit is a combination of Pennsylvanian Madera Group and Sandia Formation, and Mississippian Arroyo Peñasco and Log Cabin Formations; these strata consist of shale, sandstone, conglomerate, and limestone; all units display considerable hydrothermal alteration, veining, faulting, fracturing, and brecciation in geothermal wells; thickness is 407 and 262 m in wells VC–1 and VC–2B, respectively (Goff and Gardner 1994); thickness is 293 m in Baca–12 well (Nielson and Hulen 1984)

PROTEROZOIC

p-Є — **Proterozoic rocks, undivided**–(*Shown in cross sections only*) Highly variable unit of granite to granodiorite, aplite, schist, gneiss, and amphibolite underlying the Jemez Mountains region (table 2 of Goff et al. 1989); top of unit displays minor to severe hydrothermal alteration in geothermal wells; VC–1 penetrated roughly 15 m of greenish-gray, molybdenite-bearing gneiss breccia; alteration minerals are illite-phengite-chlorite-quartz-pyrite-calcite (Hulen and Nielson 1988); in VC–2B consists of 204 m of gray to green to pink, coarse-grained, biotite quartz monzonite; alteration minerals are epidote-illite-phengite-chlorite-quartz-pyrite-calcite; in Baca–12 consists of 90 m of white, medium-grained quartz monzonite containing epidote-chlorite-pyrite-actinolite-quartz-calcite (Nielson and Hulen 1984); age is 1.62–1.44 Ga (Rb-Sr; Brookins and Laughlin 1983)

References

All references cited in the text and the Description of Map Units, pages 17–26, are included in the following list.

Acocella, V., 2007, Understanding caldera structure and development: an overview of analogue models compared to natural calderas: Earth Science Reviews, v. 85, pp. 125–160.

Anschuetz, K. F., and Merlan, T., 2007, More than a scenic mountain landscape: Valles Caldera National Preserve land use history: U.S. Department of Agriculture, Forest Service, Rocky Mountain Research Station, Gen. Tech. Report RMRS-GTR-196, 277 pp.

Aprea, C. M., Hildebrande, S., Fehler, M., Steck, L., Baldridge, W. S., Roberts, P., Thurber, C. H., and Lutter, W. J., 2002, Three-dimensional Kirchoff migration: imaging the Jemez volcanic field using teleseismic data: Journal of Geophysical Research, v. 107, no. B102247, doi: 10.1029/2000JB000097.

Bailey, R., Smith, R., and Ross, C., 1969, Stratigraphic nomenclature of volcanic rocks in the Jemez Mountains, New Mexico: U.S. Geological Survey, Bulletin 1274-P, 19 pp.

Baugh, T. G., and Nelson, Jr., F. W., 1987, New Mexico obsidian sources and exchange on the southern Plains: Journal of Field Archaeology, v. 14, pp. 313–329.

Bethke, P. M., and Rye, R. D., 1979, Environment of ore deposition in the Creede mining district, San Juan Mountains, Colorado: Part IV, Source of fluids from oxygen, hydrogen, and carbon isotope studies: Economic Geology, v. 74, pp. 1832–1851.

Blagbrough, J. W., 1994, Late Wisconsin climatic inferences from rock glaciers in south-central and west-central New Mexico and east-central Arizona: New Mexico Geology, v. 16, no. 4, pp. 65–71.

Brookins, D., and Laughlin, A. W., 1983, Rb-Sr geochronologic investigation of Precambrian samples from deep geothermal drill holes, Fenton Hill, New Mexico: Journal of Volcanology and Geothermal Research, v. 15, pp. 43–58.

Brown, D. W., and Duchane, D. V., 1999, Scientific progress on the Fenton Hill HDR project since 1983: Geothermics, v. 28, pp. 591–601.

Broxton, D., and Reneau, S., 1995, Stratigraphic nomenclature of the Bandelier Tuff for the environmental restoration project at Los Alamos National Laboratory: Los Alamos National Laboratory, Report LA-13010-MS, 21 pp.

Broxton, D., WoldeGabriel, G., Peters, L., Budahn, J., and Luedemann, G., 2007, Pliocene volcanic rocks of the Tschicoma Formation, east-central Jemez volcanic field: Chemistry, petrography, and age constraints; *in* Kues, B., Kelley, S., and Lueth, V. (eds.), Geology of the Jemez region II: New Mexico Geological Society, Guidebook 58, pp. 284–295.

Bundy, W. M., 1958, Wall-rock alteration in the Cochiti mining district, New Mexico: New Mexico Bureau of Mines and Mineral Resources, Bulletin 59, 71 pp., maps.

Charles, R., Vidale, R., and Goff, F., 1986, An interpretation of the alteration assemblages at Sulphur Springs, Valles caldera, New Mexico: Journal of Geophysical Research, v. 91, pp. 1887–1898.

Chipera, S. J., Goff, F., Goff, C. J., and Fittapaldo, M., 2007, Zeolitization of intracaldera sediments and rhyolitic rocks in the Valles caldera, New Mexico; *in* Kues, B., Kelley, S., and Lueth, V. (eds.), Geology of the Jemez region II: New Mexico Geological Society, Guidebook 58, pp. 373–381.

Cole, J. W., Milner, D. M., Spinks, K. D., 2005, Calderas and caldera structures: a review: Earth Science Reviews, v. 69, pp. 1–26.

Conover, C. S., Theis, C. V., and Griggs, R. L., 1963, Geology and hydrology of Valle Grande and Valle Toledo, Sandoval County, New Mexico: U.S. Geological Survey, Water-Supply Paper 1619-Y, 37 pp., appendices and maps.

Davis, O. K., 1998, Palynological evidence for vegetation cycles in a 1.5 million year pollen record from the Great Salt Lake, Utah, USA: Palaeogeography, Palaeoclimatology, Palaeoecology, v. 138, pp. 175–185.

Doell, R. R., Dalrymple, G. B., Smith, R. L. and Bailey, R. A., 1968, Paleomagnetism, potassium-argon ages and geology of rhyolites and associated rocks of the Valles caldera, New Mexico; *in* Studies in volcanology—a memoir in honor of Howell Williams: Geological Society of America, Memoir 116, pp. 211–248.

Dondanville, R. F., 1978, Geologic characteristics of the Valles caldera geothermal system: Geothermal Resources Council, Transactions, v. 2, pp. 157–160.

Donohoo-Hurley, L., Geissman, J. W., Fawcett, P., Wawrzyniec, T., and Goff, F., 2007, A 200 kyr Pleistocene lacustrine record from the Valles caldera: insight from environmental magnetism and paleomagnetism; *in* Kues, B., Kelley, S., and Lueth, V. (eds.), Geology of the Jemez region II: New Mexico Geological Society, Guidebook 58, pp. 424–432.

Elston, W. E., 1994, Siliceous volcanic centers as guides to mineral exploration: review and summary: Economic Geology, v. 89, pp. 1662–1686.

Fawcett, P. J., Heikoop, J., Goff, F., Anderson, R. S., Donohoo-Hurley, L., Geissman, J. W., WoldeGabriel, G., Allen, C. D., Johnson, C. M., Smith, S. J., and Fessenden-Rahn, J., 2007, Two middle Pleistocene glacial-interglacial cycles from the Valle Grande, Jemez Mountains, northern New Mexico; *in* Kues, B., Kelley, S., and Lueth, V. (eds.), Geology of the Jemez region II: New Mexico Geological Society, Guidebook 58, pp. 409–417.

Fawcett, P. J., Werne, J. P., Anderson, R. S., Heikoop, J. M., Brown, E. T., Berke, M. A., Smith, S. J., Goff, F., Donohoo-Hurley, L., Cisneros-Dozal, L. M., Schouten, S., Sinninghe Damsté, J. S., Huang, Y., Toney, J., Fessenden, J., WoldeGabriel, G., Atudorei, V., Geissman, J. W., and Allen, C. D., 2011, Extended megadroughts in the southwestern United States during Pleistocene interglacials: Nature, v. 470, no. 7335, pp. 518–521, doi: 10.1038/nature09839.

Gardner, J. N., and Goff, F., 1984, Potassium-argon dates from the Jemez volcanic field: implications for tectonic activity in the north-central Rio Grande rift; *in* Baldridge, W. S., Dickerson, P. W., Riecker, R. E., and Zidek, Z. (eds.), Rio Grande rift: northern New Mexico: New Mexico Geological Society, Guidebook 35, pp. 75–81.

Gardner, J. N., and Goff, F., 1996, Geology of the northern Valles caldera and Toledo embayment; *in* Goff, F., Kues, B. S., Rogers, M. A., McFadden, L. D., and Gardner, J. N. (eds.), The Jemez Mountains region: New Mexico Geological Society, Guidebook 47, pp. 225–230.

Gardner, J., Goff, F., Garcia, S., and Hagan, R., 1986, Stratigraphic relations and lithologic variations in the Jemez volcanic field, New Mexico: Journal of Geophysical Research, v. 91, pp. 1763–1778.

Gardner, J. N., Goff, F., Kelley, S. A., and Jacobs, E., 2010, Rhyolites and associated deposits of the Valles–Toledo caldera complex: New Mexico Geology, v. 32, no. 1, pp. 3–18.

Gardner, J. N., Sandoval, M. M., Goff, F., Phillips, E., and Dickens, A., 2007, Geology of the Cerro del Medio moat rhyolite center, Valles caldera, New Mexico; *in* Kues, B., Kelley, S., and Lueth, V. (eds.), Geology of the Jemez region II: New Mexico Geological Society, Guidebook 58, pp. 367–372.

Gardner, J., Goff, F., Goff, S., Maassen, L., Mathews, K., Wachs, D., and Wilson, D., 1987, Core lithology, Valles Caldera #1, New Mexico: Los Alamos National Laboratory, Report LA-10957-OBES, 273 pp.

Gardner, J. N., Goff, F., Reneau, S. L., Sandoval, M. M., Drakos, P. G., Katzman, D., and Goff, C. J., 2006, Preliminary geologic map of the Valle Toledo quadrangle, Los Alamos and Sandoval Counties, New Mexico: New Mexico Bureau of Geology and Mineral Resources, Open-file Geologic Map 133, scale 1:24,000, online at http://geoinfo.nmt.edu/publications/maps/geologic/ofgm/details.cfml?Volume=133. Accessed January 11, 2011.

Gardner, J. N., Hulen, J. B., Lysne, P., Jacobson, R., Goff, F., Pisto, L., Criswell, C. W., Gribble, R., Meeker, K., Musgrave, J. A., Smith, T., Wilson, D., and Nielson, D. L., 1989, Scientific core hole Valles Caldera #2b (VC-2B), New Mexico: Drilling and some initial results: Geothermal Resources Council, Transactions, v. 13, pp. 133-139.

Geissman, J. W., 1988, Paleomagnetism and rock magnetism of Quaternary volcanic rocks and late Paleozoic strata, VC-1 core hole, Valles caldera, New Mexico, with emphasis on remagnetization of late Paleozoic strata: Journal of Geophysical Research, v. 93, pp. 6001–6025.

Gérard, A., Genter, A., Kohl, T., Lutz, P., Rose, P., and Rummel, F., editors, 2006, Special Issue: The deep EGS (Enhanced Geothermal System) Project at Soultz-sous-Forêts (Alsace, France): Geothermics, v. 35, pp. 473–710.

Glascock, M. D., Kunselman, R., and Wolfman, D., 1999, Intrasource chemical differentiation of obsidian in the Jemez Mountains and Taos Plateau, New Mexico: Journal of Archaeological Science, v. 26, pp. 861–868.

Glen, W., 1982, The road to Jaramillo: critical years of the revolution in earth science: Stanford University Press, Stanford, 479 pp.

Goff, F., 1983, Subsurface structure of Valles caldera, a resurgent cauldron in northern New Mexico (abs): Geological Society of America, Abstracts with Programs, v. 15, p. 381.

Goff, F., and Gardner, J. N., 1994, Evolution of a mineralized geothermal system, Valles caldera, New Mexico: Economic Geology, v. 89, pp. 1803–1832.

Goff, F., and Gardner, J. N., 2004, Late Cenozoic geochronology of volcanism and mineralization in the Jemez Mountains and Valles caldera, north-central New Mexico; *in* Mack, G., and Giles, K. (eds.), The geology of New Mexico: New Mexico Geological Society, Special Publication 11, pp. 295–312.

Goff, F., and Grigsby, C. O., 1982, Valles caldera geothermal systems, New Mexico, U.S.A: Journal of Hydrology, v. 56, pp. 119–136.

Goff, F., Gardner, J. N., and Valentine, G., 1990, Geology of St. Peter's Dome area, Jemez Mountains, New Mexico: New Mexico Bureau of Mines and Mineral Resources, Geologic Map 69, scale 1:24,000, 2 sheets.

Goff, F., Gardner, J. N., Reneau, S. L., and Goff, C. J., 2006a, Preliminary geologic map of the Redondo Peak quadrangle, Sandoval County, New Mexico: New Mexico Bureau of Geology and Mineral Resources, Open-file Geologic Map 111, scale 1:24,000, online at http://geoinfo.nmt.edu/publications/maps/geologic/ofgm/details.cfml?Volume=111. Accessed January 11, 2011.

Goff, F., Gardner, J., Vidale, R., and Charles, R., 1985, Geochemistry and isotopes of fluids from Sulphur Springs, Valles caldera, New Mexico: Journal of Volcanology and Geothermal Research, v. 23, pp. 273–297.

Goff, F., Shevenell, L., Gardner, J. N., Vuataz, F.-D., and Grigsby, C. O., 1988, The hydrothermal outflow plume of Valles caldera, New Mexico, and a comparison with other outflow plumes: Journal of Geophysical Research, v. 93, pp. 6041–6058.

Goff, F., Reneau, S. L., Goff, C. J., Gardner, J. N., Drakos, P. and Katzman, D., 2006b, Preliminary geologic map of the Valle San Antonio quadrangle, Sandoval County, New Mexico: New Mexico Bureau of Geology and Mineral Resources, Open-file Geologic Map 132, scale 1:24,000, online at http://geoinfo.nmt.edu/publications/maps/geologic/ofgm/details.cfml?Volume=132. Accessed January 13, 2011.

Goff, F., Warren, R. G., Goff, C. J., Whiteis, J., Kluk, E., and Counce, D., 2007, Comments on the geology, petrography, and chemistry of rocks within the resurgent dome area, Valles caldera, New Mexico; *in* Kues, B., Kelley, S., and Lueth, V. (eds.), Geology of the Jemez region II: New Mexico Geological Society, Guidebook 58, pp. 354–366.

Goff F., Goff, C. J., Phillips, E., Kyle, P., McIntosh, W., Chipera, S., and Gardner, J. N., 2003, Megabreccias, early lakes, and duration of resurgence recorded in Valles caldera, New Mexico (abs.): Transactions of American Geophysical Union (EOS), v. 84, no. 46, pp. F1649–1650.

Goff, F., Heiken, G. H., Tamanyu, S., Gardner, J. N., Self, S., Drake, R., and Shafiqullah, M., 1984, Location of Toledo caldera and formation of the Toledo embayment, Jemez Mountains, New Mexico (abs.): Transactions of American Geophysical Union (EOS), v. 65, p. 1145.

Goff, F, Reneau, S. L, Lynch, S., Goff, C. J., Gardner, J. N., Drakos, P., and Katzman, D., 2005, Preliminary geologic map of the Bland quadrangle, Los Alamos and Sandoval Counties, New Mexico: New Mexico Bureau Geology and Mineral Resources, Open-file Geologic Map 112, scale 1:24,000, online at http://geoinfo.nmt.edu/publications/maps/geologic/ofgm/details.cfml?Volume=112. Accessed January 13, 2011.

Goff, F., Gardner, J. N., Baldridge, W. S., Hulen, J. B., Nielson, D. L., Vaniman, D., Heiken, G., Dungan, M. A., and Broxton, D., 1989, Excursion 17B: Volcanic and hydrothermal evolution of Valles caldera and Jemez volcanic field; *in* Chapin, C. E., and Zidek, J. (eds.), Field excursions to volcanic terranes in the western United States, Volume I: Southern Rocky Mountain region: New Mexico Bureau of Mines and Mineral Resources, Memoir 46, pp. 381–434.

Goldstein, N. E., and Tsang, C. F., 1984, A review of lessons learned from the DOE/Union Baca geothermal project: Geothermal Resources Council, Bulletin, June 1984, pp. 7–11.

Grant, M. A., Garg, S. K., and Riney, T. D., 1984, Interpretation of downhole data and development of a conceptual model for the Redondo Creek area of the Baca geothermal field: Water Resources Research, v. 20, pp. 1401–1416.

Griggs, R., 1964, Geology and groundwater resources of the Los Alamos area, New Mexico: U.S. Geological Survey, Water-Supply Paper 1753, 107 pp. (1:24,000-scale map).

Heiken, G., Murphy, H., Nunz, G., Potter, R., and Grigsby, C., 1981, Hot dry rock geothermal energy: American Scientist, v. 69, pp. 400–407.

Heiken, G., Goff, F., Stix, J., Tamanyu, S., Shafiqullah, M., Garcia, S., and Hagan, R., 1986, Intracaldera volcanic activity, Toledo caldera and embayment, Jemez Mountains, New Mexico: Journal of Geophysical Research, v. 91, pp. 1799–1815.

Hulen, J. B., and Gardner, J. N., 1989, Field geologic log for Continental Scientific Drilling Program corehole VC-2B, Valles caldera, New Mexico: Earth Science Laboratory, University of Utah Research Institute, Salt Lake City, Report DOE/ER/13196-4, ESL-89025-TR, 92 pp.

Hulen, J. B., and Nielson, D., 1986, Hydrothermal alteration in the Baca geothermal system, Redondo dome, Valles caldera, New Mexico: Journal of Geophysical Research, v. 91, pp. 1867–1886.

Hulen, J. B., and Nielson, D., 1988, Hydrothermal brecciation in the Jemez fault zone, Valles caldera, New Mexico: results from Continental Scientific Drilling Program corehole VC-1: Journal of Geophysical Research, v. 93, pp. 6077–6091.

Hulen, J. B., Nielson, D. L., and Little, T. M., 1991, Evolution of the western Valles caldera complex, New Mexico: evidence from intracaldera sandstones, breccias, and surge deposits: Journal of Geophysical Research, v. 96, no. B5, pp. 8127–8142.

Hulen, J. B., Nielson, D. L., Goff, F., Gardner, J. N., and Charles, R., 1987, Molybdenum mineralization in an active geothermal system, Valles caldera: New Mexico. Geology, v. 15, pp. 748–752.

Izett, G. A., and Obradovich, J. D., 1994, $^{40}Ar/^{39}Ar$ age constraints for the Jaramillo Normal Subchron and the Matuyama–Brunhes geomagnetic boundary: Journal of Geophysical Research, v. 99, pp. 2925–2934.

Justet, L., 2003, Effects of basalt intrusion on the multi-phase evolution of the Jemez volcanic field, New Mexico: Unpublished Ph.D. dissertation, University of Nevada, Las Vegas, 246 pp.

Justet, L., and Spell, T. L., 2001, Effusive eruptions from a large silicic magma chamber: the Bearhead Rhyolite, Jemez volcanic field, New Mexico: Journal of Volcanology and Geothermal Research, v. 107, pp. 241–264.

Kelley, S. A., Kempter, K. A., and Lawrence, J. R., 2007a, Stratigraphic nomenclature and trends in volcanism in the northern Jemez Mountains; *in* Kues, B., Kelley, S., and Lueth, V. (eds.), Geology of the Jemez region II: New Mexico Geological Society, Guidebook 58, pp. 48–49.

Kelley, S. A., Osburn, G. R., and Kempter, K. A., 2007b, Geology of Cañon de San Diego, southwestern Jemez Mountains, north-central New Mexico; *in* Kues, B., Kelley, S., and Lueth, V. (eds.), Geology of the Jemez region II: New Mexico Geological Society, Guidebook 58, pp. 169–181.

Kelley, S., Osburn, G. R., Ferguson, C., Kempter, K., and Osburn, M., 2004, Preliminary geologic map of the Seven Springs 7.5-minute quadrangle, Rio Arriba and Sandoval Counties, New Mexico: New Mexico Bureau of Geology and Mineral Resources, Open-file Geologic Map 88, scale 1:24,000, online at http://geoinfo.nmt.edu/publications/maps/geologic/ofgm/details.cfml?Volume=88. Accessed January 13, 2011.

Kelley, S., Kempter, K. A., Goff, F., Rampey, M., Osburn, G. R., and Ferguson, C. A., 2003, Geology of the Jemez Springs 7.5-minute quadrangle, Sandoval County, New Mexico: New Mexico Bureau of Geology and Mineral Resources, Open-file Geologic Map 73, scale 1:24,000, online at http://geoinfo.nmt.edu/publications/maps/geologic/ofgm/details.cfml?Volume=73. Accessed January 13, 2011.

Kempter, K. A., Kelley, S. A., and Lawrence, J. R., 2007, Geology of the northern Jemez Mountains, north-central New Mexico; *in* Kues, B., Kelley, S., and Lueth, V. (eds.), Geology of the Jemez region II: New Mexico Geological Society, Guidebook 58, pp. 155–168.

Kempter, K. A., Kelley, S. A., Kelley, S., and Fluk, L., 2004, Preliminary geologic map of the Polvadera Peak 7.5-minute quadrangle, Rio Arriba and Sandoval Counties, New Mexico: New Mexico Bureau of Geology and Mineral Resources, Open-file Geologic Map 96, scale 1:24,000, online at http://geoinfo.nmt.edu/publications/maps/geologic/ofgm/details.cfml?Volume=96. Accessed January 13, 2011.

Kennedy, B., Stix, J., Vallance, J. W., Lavellèe, Y., Longprè, M. A., 2004, Controls on caldera structure: results from analogue sandbox modeling: Geological Society of America, Bulletin, v. 106, pp. 515–524.

Kerr, R. A., 1982, Extracting geothermal energy can be hard: Science, v. 218, pp. 668–669.

Kerr, R. A., 1987, Hot dry rock: Problems, promise: Science, v. 238, pp. 1226–1228.

Lambert, S. J., and Epstein, S., 1980, Stable isotope investigations of an active geothermal system in the Valles caldera, Jemez Mountains, New Mexico: Journal of Volcanology and Geothermal Research, v. 8, pp. 111–129.

Laughlin, A. W., Eddy, A. C., Laney, R., and Aldrich, M. J., 1983, Geology of the Fenton Hill, New Mexico, hot dry rock site: Journal of Volcanology and Geothermal Research, v. 15, pp. 21–41.

Lawrence, J. R., 2007, Stratigraphy and geochronology of mafic to intermediate volcanic rocks of La Grulla Plateau, northwestern Jemez Mountains; *in* Kues, B., Kelley, S., and Lueth, V. (eds.), Geology of the Jemez region II: New Mexico Geological Society, Guidebook 58, pp. 46–47.

Lawrence, J. R., Kelley, S., and Rampey, M., 2004, Preliminary geologic map of the Cerro del Grant 7.5-minute quadrangle, Rio Arriba and Sandoval Counties, New Mexico: New Mexico Bureau of Geology and Mineral Resources, Open-file Geologic Map 87, scale 1:24,000, online at http://geoinfo.nmt.edu/publications/maps/geologic/ofgm/details.cfml?Volume=87. Accessed January 13, 2011.

Lepper, K., and Goff, F., 2007, Yet another attempt to date the Banco Bonito rhyolite, the youngest volcanic flow in the Valles caldera, New Mexico: New Mexico Geology, v. 29, pp. 117–121.

Lepper, K., Reneau, S. L., Thorstad, J., and Denton, A., 2007, OSL dating of a lacustrine to fluvial transitional sediment sequence in Valle Toledo, Valles caldera, New Mexico: New Mexico Geology, v. 29, pp. 112–116.

Lipman, P. W., 1976, Caldera collapse breccias in the southern San Juan Mountains, Colorado: Geological Society of America, Bulletin, v. 87, pp. 1397–1410.

Lipman, P. W., 2000, Calderas; *in* Sigurdsson, H., Houghton, B., McNutt, S., Rymer, H., Stix, J. (eds.), Encyclopedia of volcanoes: Academic Press, San Diego, pp. 643–662.

Loeffler, B., Vaniman, D., Baldridge, W., and Shafiqullah, M., 1988, Neogene rhyolites of the northern Jemez volcanic field, New Mexico: Journal of Geophysical Research, v. 93, pp. 6157–6167.

Lysne, P., and Jacobson, R., 1990, Scientific drilling in hydrothermal terraines: Scientific Drilling, v. 1, pp. 184–192.

Marti, J., Ablay, G. J., Redshaw, I. T., and Sparks, R. S. J., 1994, Experimental studies of caldera collapse: Journal of the Geological Society, v. 151, pp. 919–929.

Martin, C., 2003, History of the Baca Location No. 1: All Seasons Publishing, Los Alamos, New Mexico, 157 pp.

Murphy, H. D., Tester, J. W., Grigsby, C. O., and Potter, R. W., 1981, Energy extraction from fractured geothermal reservoirs in low-permeability crystalline rock: Journal of Geophysical Research, v. 86, pp. 7145–7158.

Nielson, D., and Hulen, J., 1984, Internal geology and evolution of the Redondo dome, Valles caldera, New Mexico: Journal of Geophysical Research, v. 89, pp. 8695–8711.

Nowell, D., 1996, Gravity modeling of the Valles caldera; *in* Goff, F., Kues, B., Rogers, M., McFadden, L., and Gardner, G. (eds.), The Jemez Mountains region: New Mexico Geological Society, Guidebook 47, pp. 121–128.

Ogoh, K., Toyoda, S., Ikeda, S., Ikeya, M., and Goff, F., 1993, Cooling history of the Valles caldera, New Mexico using ESR dating method: Applied Radiation Isotropy, v. 44, pp. 233–237.

Phillips, E. H., 2004, Collapse and resurgence of the Valles caldera, Jemez Mountains, New Mexico: $^{40}Ar/^{39}Ar$ age constraints on the timing and duration of resurgence and ages of megabreccia blocks: Unpublished M.S. thesis, New Mexico Institute of Mining and Technology, Socorro, 200 pp.

Phillips, E. H., Goff, F., Kyle, P. R., McIntosh, W. C., Dunbar, N. W., and Gardner, J. N., 2007, The $^{40}Ar/^{39}Ar$ age constraints on the duration of resurgence at the Valles caldera, New Mexico: Journal of Geophysical Research, v. 112, B08201, 15 pp.

Phillips, W., Poths, J., Goff, F., Reneau, S., and McDonald, E., 1997, Ne-21 surface exposure ages from the Banco Bonito obsidian flow, Valles caldera, New Mexico, USA (abs.), Geological Society of America, Abstracts with Programs, v. 29, no. 6, p. A-419.

Reneau, S. L., Drakos, P. G., and Katzman, D., 2007, Post-resurgence lakes in the Valles caldera, New Mexico; *in* Kues, B., Kelley, S., and Lueth, V. (eds.), Geology of the Jemez region II: New Mexico Geological Society, Guidebook 58, pp. 398–408.

Reneau, S., Gardner, J., and Forman, S., 1996, New evidence for the age of the youngest eruptions in the Valles caldera: Geology, v. 24, pp. 7–10.

Rogers, J. B., Smith, G. A., and Rowe, H., 1996, History of formation and drainage of Pleistocene lakes in the Valles caldera; *in* Goff, F., Kues, B. S., Rogers, M. A., McFadden, L. D., and Gardner, J. N. (eds.), The Jemez Mountains region: New Mexico Geological Society, Guidebook 47, pp. 14–16.

Rowe, M. C., Wolff, J. A., Gardner, J. N., Ramos, F. C., Teasdale, R., and Heikoop, C. E., 2007, Development of a continental volcanic field: Petrogenesis of pre-caldera intermediate and silicic rocks and origin of the Bandelier magmas, Jemez Mountains (New Mexico, USA): Journal of Petrology, v. 48, pp. 2063–2091.

Rubin, A. R., 1992, Dike-induced faulting and graben subsidence in volcanic rift zones: Journal of Geophysical Research, v. 97, pp. 1839–1858.

Sasada, M., and Goff, F., 1995, Fluid inclusion evidence for rapid formation of the vapor-dominated zone at Sulphur Springs, Valles caldera, New Mexico, USA: Journal of Volcanology and Geothermal Research, v. 67, pp. 161–169.

Sass, J. H., and Morgan, P., 1988, Conductive heat flux in VC-1 and the thermal regime of Valles caldera, Jemez Mountains, New Mexico: Journal of Geophysical Research, v. 93, pp. 6027–6039.

Sears, P. B., and Clisby, K. H., 1952, Two long climate records: Science, v. 116, pp. 176–178.

Segar, R., 1974, Quantitative gravity interpretation, Valles caldera area, Sandoval and Rio Arriba Counties, New Mexico: University of Utah Research Institute, Earth Science Laboratory, Open-file Report, NM/BACA-27, 12 pp.

Self, S., Kircher, D. E., and Wolff, J. A., 1988, The El Cajete Series, Valles caldera, New Mexico: Journal of Geophysical Research, v. 93, pp. 6113–6127.

Self, S., Goff, F., Gardner, J., Wright, J., and Kite, W., 1986, Explosive rhyolitic volcanism in the Jemez Mountains: vent locations, caldera development, and relation to regional structure: Journal of Geophysical Research, v. 91, pp. 1779–1798.

Shackley, M. S., 2005, Obsidian: geology and archaeology in the North American Southwest: University of Arizona Press, Tucson, 246 pp.

Sillitoe, R. H., and Bonham, H. F., Jr., 1984, Volcanic landforms and ore deposits: Economic Geology, v. 79, pp. 1286–1298.

Singer, B., and Brown, L., 2002, The Santa Rosa event: $^{40}Ar/^{39}Ar$ and paleomagnetic results from the Valles Rhyolite near Jaramillo Creek, Jemez Mountains, New Mexico: Earth and Planetary Science Letters, v. 197, pp. 51–64.

Smith, G. A., and Lavine, A., 1996, What is the Cochiti Formation? *in* Goff, F., Kues, B. S., Rogers, M. A., McFadden, L. D., and Gardner, J. N. (eds.), The Jemez Mountains region: New Mexico Geological Society, Guidebook 47, pp. 219–224.

Smith, R. L., 1960, Ash flows: Geological Society of America, Bulletin, v. 71, pp. 795–842.

Smith, R. L., and Bailey, R. A., 1966, The Bandelier Tuff: a study of ash-flow eruption cycles from zoned magma chambers: Bulletin of Volcanology, v. 29, pp. 83–104.

Smith, R. L., and Bailey, R. A., 1968, Resurgent cauldrons: Geological Society of America, Memoir 116, pp. 613–662.

Smith, R. L., Bailey, R. A., and Ross, C. S., 1961, Structural evolution of the Valles caldera, New Mexico, and its bearing on the emplacement of ring dikes: U.S. Geological Survey, Professional Paper 424-D, pp. D145–D149.

Smith, R. L., Bailey, R. A., and Ross, C. S., 1970, Geologic map of the Jemez Mountains, New Mexico: U.S. Geological Survey, Miscellaneous Geologic Investigations Map I-571, 1:125,000 scale.

Spell, T. L., and Harrison, T. M., 1993, $^{40}Ar/^{39}Ar$ geochronology of post-Valles caldera rhyolites, Jemez volcanic field, New Mexico: Journal of Geophysical Research, v. 98, pp. 8031–8051.

Spell, T. L., Harrison, T. M., and Wolff, J. A., 1990, $^{40}Ar/^{39}Ar$ dating of the Bandelier Tuff and San Diego Canyon ignimbrites, Jemez Mountains, New Mexico: temporal constraints on magmatic evolution: Journal of Volcanology and Geothermal Research, v. 43, pp. 175–193.

Spell, T. L., McDougall, I., and Doulgeris, A., 1996, Cerro Toledo Rhyolite, Jemez volcanic field, New Mexico: $^{40}Ar/^{39}Ar$ geochronology of eruptions between two caldera-forming events: Geological Society of America, Bulletin, v. 108, pp. 1549–1566.

Steck, L. K., Thurber, C. H., Fehler, M. C., Lutter, W. J., Roberts, P. M., Baldridge, W. S., Stafford, D. G., and Sessions, R., 1998, Crust and upper mantle P wave velocity structure beneath Valles caldera, New Mexico: results from the Jemez teleseismic tomography experiment: Journal of Geophysical Research, v. 103, pp. 24,301–24,302.

Steffen, A., 2005, The Dome Fire obsidian study: investigating the interaction of heat, hydration, and glass geochemistry: Unpublished Ph.D. dissertation, University of New Mexico, Albuquerque, 386 pp.

Stein, H. L., 1983, Geology of the Cochiti mining district, Jemez Mountains, New Mexico: Unpublished M.S. thesis, University of New Mexico, Albuquerque, 122 pp.

Stix, J., Goff, F., Gorton, M. P., Heiken, G., and Garcia, S. R., 1988, Restoration of compositional zonation in the Bandelier silicic magma chamber between two caldera-forming eruptions: geochemistry and origin of the Cerro Toledo Rhyolite, Jemez Mountains, New Mexico: Journal of Geophysical Research, v. 93, pp. 6129–6147.

Summers, W. K., 1976, Catalog of thermal waters in New Mexico: New Mexico Bureau of Mines and Mineral Resources, Hydrologic Report 4, 80 pp.

Timmer, R., Woodward, L., Kempter, K., Kelley, S., Osburn, R., Osburn, M., Buffler, R., and Lawrence, J. R., 2006, Preliminary geologic map of the Jarosa quadrangle, Rio Arriba County, New Mexico: New Mexico Bureau of Geology and Mineral Resources, Open-file Geologic Map 128, scale 1:24,000, online at http://geoinfo.nmt.edu/publications/maps/geologic/ofgm/details.cfml?Volume=128. Accessed January 12, 2011.

Toyoda, S., Goff, F., Ikeda, S., and Ikeya, M., 1995, ESR dating of quartz phenocrysts in the El Cajete and Battleship Rock Members of Valles Rhyolite, Valles caldera, New Mexico: Journal of Volcanology and Geothermal Research, v. 67, pp. 29–40.

Truesdell, A. H., and Janik, C. J., 1986, Reservoir processes and fluid origins in the Baca geothermal system, Valles caldera, New Mexico: Journal of Geophysical Research, v. 91, pp. 1817–1833.

Vezzoli, L., Principe, C., Malfatti, J., Arrighi, S., Tanguy, J.-C., and Le Goff, M., 2009, Modes and times of caldera resurgence: The <10 ka evolution of Ischia caldera, Italy, from high-precision archeomagnetic dating: Journal of Volcanology and Geothermal Research, v. 186, pp. 305–329.

Warren, R. G., Goff, F., Kluk, E. C., and Budahn, J. R., 2007, Petrography, chemistry, and mineral compositions for subunits of the Tshirege Member, Bandelier Tuff within the Valles caldera and Pajarito Plateau; *in* Kues, B., Kelley, S., and Lueth, V. (eds.), Geology of the Jemez region II: New Mexico Geological Society, Guidebook 58, pp. 316–332.

Warshaw, C., and Smith, R. L., 1988, Pyroxenes and fayalites in the Bandelier Tuff, New Mexico: temperatures and comparison with other rhyolites: American Mineralogist, v. 73, pp. 1025–1037.

White, D. E., 1955, Thermal springs and epithermal ore deposits: Economic Geology, 50th Anniversary Volume, pp. 99–154.

WoldeGabriel, G., 1990, Hydrothermal alteration in the Valles caldera ring fracture zone and core hole VC-1: evidence for multiple hydrothermal systems: Journal of Volcanology and Geothermal Research, v. 40, pp. 105–122.

WoldeGabriel, G., and Goff, F., 1989, Temporal relationships of volcanism and hydrothermal systems in two areas of the Jemez volcanic field, New Mexico: Geology, v. 17, pp. 986–989.

WoldeGabriel, G., and Goff, F., 1992, K/Ar dates of hydrothermal clays from VC-2B, Valles caldera, New Mexico, and their relation to alteration in a large hydrothermal system: Journal of Volcanology and Geothermal Research, v. 50, pp. 207–230.

Wolff, J. A., and Gardner, J. N., 1995, Is the Valles caldera entering a new cycle of activity? Geology, v. 23, pp. 411–414.

Wolff, J. A., Brunstad, K. A., and Gardner, J. N., 2011, Reconstruction of the most recent volcanic eruptions fron the Valles caldera, New Mexico: Journal of Volcanology and Geothermal Research, v. 199, pp. 53–68, doi: 10.1016/jvolgeores.2010.10.008.

Wolff, J. A., Rowe, M. C., Teasdale, R., Gardner, J. N., Ramos, F. C., and Heikoop, C. E., 2005, Petrogenesis of pre-caldera mafic lavas, Jemez Mountains volcanic field (New Mexico, USA): Journal of Petrology, v. 46, pp. 407–439.